Agonist-Independent Constitutive Activity of Angiotensin II Receptor Promotes Cardiac Remodeling in Mice

Noritaka Yasuda, Hiroshi Akazawa, Kaoru Ito, Ippei Shimizu, Yoko Kudo-Sakamoto, Chizuru Yabumoto, Masamichi Yano, Rie Yamamoto, Yukako Ozasa, Tohru Minamino, Atsuhiko T. Naito, Toru Oka, Ichiro Shiojima, Kouichi Tamura, Satoshi Umemura, Pierre Paradis, Mona Nemer, Issei Komuro

See Editorial Commentary, pp 542–544

Abstract—The angiotensin II (Ang II) type 1 (AT_1) receptor mainly mediates the physiological and pathological actions of Ang II, but recent studies have suggested that AT_1 receptor inherently shows spontaneous constitutive activity even in the absence of Ang II in culture cells. To elucidate the role of Ang II–independent AT_1 receptor activation in the pathogenesis of cardiac remodeling, we generated transgenic mice overexpressing AT_1 receptor under the control of α-myosin heavy chain promoter in angiotensinogen-knockout background (AT_1Tg-AgtKO mice). In AT_1Tg-AgtKO hearts, redistributions of the $G\alpha_{q11}$ subunit into cytosol and phosphorylation of extracellular signal-regulated kinases were significantly increased, compared with angiotensinogen-knockout mice hearts, suggesting that the AT_1 receptor is constitutively activated independent of Ang II. As a consequence, AT_1Tg-AgtKO mice showed spontaneous systolic dysfunction and chamber dilatation, accompanied by severe interstitial fibrosis. Progression of cardiac remodeling in AT_1Tg-AgtKO mice was prevented by treatment with candesartan, an inverse agonist for the AT_1 receptor, but not by its derivative candesartan-7H, deficient of inverse agonism attributed to a lack of the carboxyl group at the benzimidazole ring. Our results demonstrate that constitutive activity of the AT_1 receptor under basal conditions contributes to the cardiac remodeling even in the absence of Ang II, when the AT_1 receptor is upregulated in the heart. (***Hypertension.* 2012;59:627-633.)** • Online Data Supplement

Key Words: ARB ■ cardiac dysfunction ■ fibrosis ■ G protein-coupled receptor ■ inverse agonist

The angiotensin II (Ang II) type 1 (AT_1) receptor is a 7 transmembrane spanning G protein-coupled receptor (GPCR), and the activation of AT_1 receptor is involved in regulating pathophysiological processes of the cardiovascular system. In principle, the AT_1 receptor is activated on binding to Ang II, which is produced systemically or locally after sequential proteolytic processing. However, recent studies demonstrated that the AT_1 receptor inherently shows spontaneous constitutive activity even in the absence of Ang II in cultured cells.[1–3] GPCRs are structurally unstable and show significant levels of spontaneous activity in an agonist-independent manner.[4] In addition, we and others demonstrated that the AT_1 receptor can be activated by mechanical stress independent of Ang II[5–7] through conformational switch of the receptor.[1] These observations have highlighted the inverse agonist activity of AT_1 receptor blockers (ARBs) as a drug-specific property that can inhibit Ang II–independent constitutive activity and mechanical stress-induced receptor activation.[1,2,5,8] In a mouse model, mechanical stress-induced AT_1 receptor activation led to the development of cardiac hypertrophy independent of Ang II, and treatment with inverse agonists for the AT_1 receptor-attenuated cardiac hypertrophy thus formed.[5] However, the pathogenic role of Ang II–independent constitutive activity of the AT_1 receptor and clinical relevance of inverse agonist activity of ARBs against constitutive receptor activation remains to be elucidated in vivo. In several GPCRs, gain-of-function mutations are causative of diseases, but any activating mutations in the

Received April 24, 2011; first decision May 23, 2011; revision accepted January 6, 2012.

From the Department of Cardiovascular Science and Medicine (N.Y., K.I., Ip.S., R.Y., Y.O., T.M.), Chiba University Graduate School of Medicine, Chiba, Japan; Departments of Cardiovascular Medicine (H.A, Y.K.-S., C.Y., M.Y., T.O., I.K.) and Cardiovascular Regenerative Medicine (A.T.N., Ic.S.), Osaka University Graduate School of Medicine, Suita, Japan; Department of Medical Science and Cardiorenal Medicine (K.T., S.U.), Yokohama City University Graduate School of Medicine, Yokohama, Japan; Lady Davis Institute for Medical Research (P.P.), Sir Mortimer B. Davis-Jewish General Hospital, McGill University, Montreal, Quebec, Canada; Laboratory of Cardiac Growth and Differentiation (M.N.), Department of Biochemistry, Microbiology, and Immunology, Faculty of Medicine, University of Ottawa, Ottawa, Ontario, Canada.

The online-only Data Supplement is available with this article at http://hyper.ahajournals.org/lookup/suppl/doi:10.1161/HYPERTENSIONAHA.111.175208/-/DC1.

Correspondence to Issei Komuro, Department of Cardiovascular Medicine, Osaka University Graduate School of Medicine, 2-2 Yamadaoka, Suita, Osaka 565-0871, Japan. E-mail komuro-tky@umin.ac.jp

Hypertension **is available at http://hyper.ahajournals.org** **DOI: 10.1161/HYPERTENSIONAHA.111.175208**

coding region of the AT_1 receptor gene have not been identified in hypertension or primary hyperaldosteronism.[9,10] Although knock-in mice with a constitutively activating mutation (substitution of Asn^{111} to Ser with a C-terminal deletion) showed low-renin hypertension and progressive fibrosis in kidney and heart,[11] it remains unclear whether constitutive activity of the native AT_1 receptor leads to some phenotypic abnormalities even under circumstances where the production of Ang II is genetically inhibited.

Therefore, we generated transgenic mice overexpressing AT_1 receptor under the control of *α-myosin heavy chain* promoter in the *angiotensinogen* (*Agt*)-knockout background. Here, we show that constitutive activity of the AT_1 receptor indeed contributes to cardiac remodeling independent of Ang II even in vivo, when the AT_1 receptor is upregulated in the heart.

Methods

An expanded Methods section is available in the online-only Data Supplement.

Mice, Transverse Aortic Constriction Operation, and Transthoracic Echocardiography

Mice expressing the human *AGTR1* gene under the control of *α-myosin heavy chain* promoter (on the C57BL/6J background) and mice deficient for the *Agt* gene (on the Institute of Cancer Research [ICR] background) were described previously.[12,13] Candesartan cilexetil and candesartan-7H were synthesized by Takeda Pharmaceutical Co, Ltd, and administered via drinking water. Sham or transverse aortic constriction operation was performed as described previously,[5] and transthoracic echocardiography was performed on conscious mice with a Vevo 770 Imaging System. All of the protocols were approved by the institutional animal care and use committee of Chiba University.

Ang II Infusion and BP Measurement

Eight-week–old C57BL/6J male mice were treated with Ang II (0.6 mg/kg per day) or vehicle for 2 weeks using an osmotic mini-pump (ALZET model 2002; Durent Corp). The BP and pulse rates were measured noninvasively by a programmable sphygmomanometer (BP-98A, Softron) using the tail-cuff method.

Real-Time RT-PCR Analysis

Total RNA was extracted by using the RNeasy kit (Qiagen), and single-stranded cDNA was transcribed by using QuantiTect Reverse Transcription kit (Qiagen), according to the manufacturer's protocol. We conducted quantitative real-time PCR analysis with the Universal ProbeLibrary Assays (Roche Applied Science), according to the manufacturer's instructions.

Western Blot Analysis and Histological Analysis

Western blot analysis and histological were performed as described previously.[1,5]

Radioligand Receptor Binding Assay

Radioligand binding assays were performed as described previously.[1,14]

Statistics

All of the data are presented as mean±SEM. Two-group comparison was analyzed by unpaired 2-tailed Student *t* test, and multiple-group comparison was performed by 1-way ANOVA followed by the Fisher protected least significant difference test for comparison of means. A *P* value of $P<0.05$ was considered to be statistically significant.

Results

AT_1 Receptor Is Constitutively Activated Without the Involvement of Ang II in AT_1 Transgenic-Angiotensinogen Knockout Mice Hearts

To elucidate the pathogenic role of Ang II–independent AT_1 receptor activation in the hearts, we crossed transgenic mice overexpressing human AT_1 receptor under the control of cardiac-specific *α-myosin heavy chain* promoter (AT_1Tg) with angiotensinogen knockout mice (AgtKO) to generate AT_1Tg-AgtKO mice. First, we examined the expression levels of renin-angiotensin system components. Although the mRNA level of the AT_2 receptor (*Agtr2*) was significantly higher in AT_1Tg-AgtKO hearts than in AgtKO hearts, there was no significant difference in protein levels of the AT_2 receptor between AT_1Tg-AgtKO and AgtKO hearts (Figure S1 in the online-only Data Supplement). Furthermore, the mRNA levels of the AT_{1b} receptor (*Agtr1b*), angiotensin-converting enzyme (*Ace*), and renin (*Ren1* and *Ren2*) did not differ significantly between AT_1Tg-AgtKO and AgtKO hearts (Figure S1A).

We next determined the density of the AT_1 receptor (B_{max} values of receptor binding) in membranes isolated from the ventricles of AgtKO and AT_1Tg-AgtKO mice by radioligand binding assays using ^{125}I-[Sar^1, Ile^8] Ang II as ligand. Consistent with the previous report,[12] the B_{max} of AT_1 receptor was increased by >200-fold in AT_1Tg-AgtKO hearts compared with AgtKO hearts (AT_1Tg-AgtKO: 5.41±1.79 pmol/mg of protein; AgtKO: 24.0±13.9 fmol/mg of protein; n=4 per group; $P<0.01$). Next, to evaluate whether the AT_1 receptor is constitutively activated in the AT_1Tg-AgtKO hearts, we examined redistribution of $G\alpha_{q11}$ into the cytosolic fraction and phosphorylation of extracellular signal–regulated kinases (ERKs) in AgtKO and AT_1Tg-AgtKO hearts. On activation of the AT_1 receptor, the heterotrimeric G_q protein dissociates into α and $\beta\gamma$ subunits, and the GTP-bound $G\alpha_q$ subunit stimulates diverse intracellular signaling pathways, including the ERK pathway.[15,16] Redistribution of $G\alpha_{q11}$ subunits from the particulate to the cytosolic fraction was significantly increased in AT_1Tg-AgtKO hearts compared with AgtKO hearts (Figure 1A). In addition, the levels of phosphorylated ERKs in AT_1Tg-AgtKO hearts was significantly increased compared with AgtKO hearts (Figure 1B). These results suggest that the AT_1 receptor is upregulated and constitutively activated without the involvement of Ang II in the AT_1Tg-AgtKO hearts.

AT_1Tg-AgtKO Mice Display Progressive Cardiac Remodeling

Tail-cuff measurements of systolic and diastolic blood pressure (BPs) and pulse rates revealed that these parameters did not differ significantly between AgtKO and AT_1Tg-AgtKO mice at 20 weeks of age (Table). However, morphological and physiological analysis revealed progressive chamber dilatation, contractile dysfunction, and interstitial fibrosis in AT_1Tg-AgtKO mice, whereas cardiac structure and function were normal in AgtKO mice. At 20 weeks of age, AT_1Tg-AgtKO mice displayed ≈1.5-fold increase in heart:body

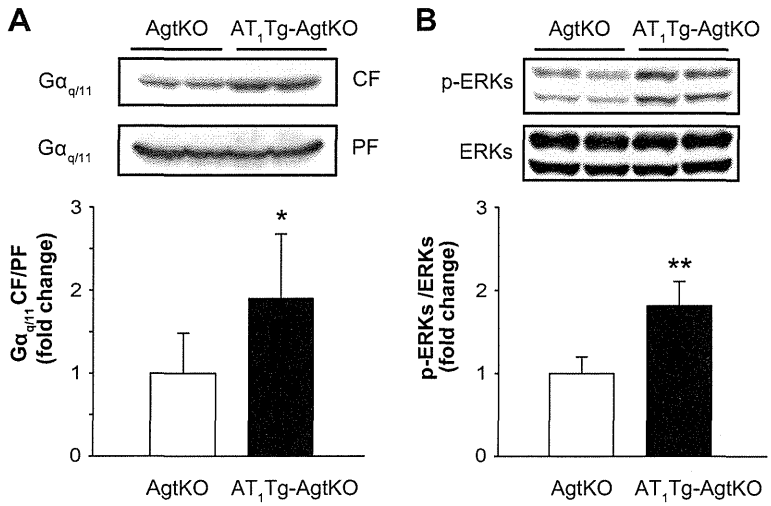

Figure 1. Constitutive activation of angiotensin II type 1 (AT_1) receptor in AT_1 transgenic (AT_1Tg)-angiotensinogen-knockout (AgtKO) hearts. **A**, Immunoblot analysis of $G\alpha_{q/11}$ in cytosolic fraction (CF) and particulate fraction (PF) extracted from AgtKO (n=6) and AT_1Tg-AgtKO (n=6) hearts. The quantitation of the $G\alpha_{q/11}$ in CF/PF is shown as a bar graph. Data are presented as mean±SEM. *$P<0.05$ vs AgtKO mice. **B**, Immunoblot analysis of phosphorylated extracellular signal–regulated kinases (ERKs; p-ERKs) and total ERKs in AgtKO (n=8) and AT_1Tg-AgtKO (n=8) hearts. The quantitation of the p-ERKs/ERKs is shown as a bar graph. Data are presented as mean±SEM. **$P<0.01$ vs AgtKO mice.

weight ratio compared with AgtKO mice (Table). Echocardiographic examination revealed a progressive increase in left ventricular end-diastolic dimension and decrease in the percentage of fractional shortening (Figure 2A). Histologically, a significant increase in interstitial fibrosis was observed in AT_1Tg-AgtKO mice at 20 weeks of age and further exacerbated at 36 weeks of age (Figure 2B). Furthermore, real-time RT-PCR indicated that mRNA levels of fetal cardiac genes (*Nppa*, *Nppb*, and *Acta1*) and extracellular matrix genes (*Col3a1* and *Postn*) were significantly increased in AT_1Tg-AgtKO hearts compared with AgtKO hearts (Figure 2C). These results indicate that upregulation of the AT_1 receptor induced spontaneous and progressive cardiac remodeling in AT_1Tg-AgtKO mice in spite of systemic deficiency of Ang II.

Cardiac Remodeling in AT_1Tg-AgtKO Mice Is Prevented by Treatment With an Inverse Agonist for the AT_1 Receptor

We examined whether an AT_1 receptor blocker candesartan could prevent the progression of cardiac remodeling in AT_1Tg-AgtKO mice. In cultured cells, candesartan reduces the basal activity of both the wild-type AT_1 receptor and constitutively active AT_1 mutant receptors, suggesting that candesartan is an inverse agonist for the AT_1 receptor.[1] Candesartan also suppresses mechanical stretch-induced helical movement and thereby inhibits receptor activation[1] and prevents pressure-overload cardiac hypertrophy in mice.[5]

Table. Measurement of Heart Weight, Heart Rate, and BP in AgtKO and AT_1Tg-AgtKO Mice at 20 wk of Age

Parameters	AgtKO	No.	AT_1Tg-AgtKO	No.
BW, g	31.0±3.4	9	30.2±3.5	6
HW/BW, mg/g	3.48±0.25	9	5.08±0.19*	6
HR, bpm	556.0±85.3	6	540.1±55.0	6
Systolic BP, mm Hg	83.4±8.8	6	85.9±3.7	6
Diastolic BP, mm Hg	57.3±6.0	6	55.7±7.4	6
Mean BP, mm Hg	65.7±5.3	6	66.0±5.0	6

BW indicates body weight; HR, heart rate; HW/BW, heart:body weight ratio; BP, blood pressure; AgtKO, angiotensinogen-knockout; AT_1Tg, angiotensin II type 1 transgenic.
*$P<0.01$ vs sham.

Tail-cuff measurements revealed a significant increase in systolic BP in 8-week–old C57BL/6 male mice treated with Ang II (0.6 mg/kg per day) for 2 weeks using an osmotic minipump (Figure 3A). This BP elevation was abolished by treatment with candesartan cilexetil (1 mg/kg per day) in drinking water. Candesartan cilexetil is a prodrug that is converted rapidly and completely to candesartan during gastrointestinal absorption.[17] Interestingly, treatment with candesartan cilexetil prevented the progression of cardiac remodeling in AT_1Tg-AgtKO mice, when treatment was initiated at 6 weeks of age. The increases in heart:body weight ratio (Figure 3B), chamber dilatation and contractile dysfunction (Figure 3C), and interstitial fibrosis (Figure 3D) were significantly attenuated by candesartan cilexetil. Consistently, real-time RT-PCR indicated that the increases in mRNA levels of fetal cardiac genes (*Nppa*, *Nppb*, and *Acta1*) and extracellular matrix genes (*Col3a1* and *Postn*) in AT_1Tg-AgtKO hearts were significantly attenuated by treatment with candesartan cilexetil (Figure 3E).

We reported previously that tight binding between the carboxyl group of candesartan and specific residues of the AT_1 receptor was critical for the potent inverse agonism and that a derivative of candesartan (candesartan-7H), lacking the carboxyl group at the benzimidazole ring, could not suppress agonist-independent activities of the receptor.[1] Although treatment with candesartan-7H (1 mg/kg per day) had no effect, treatment with candesartan-7H (20 mg/kg per day) suppressed Ang II–induced BP elevation in C57BL/6 male mice, almost equally as treatment with candesartan cilexetil (1 mg/kg per day) did. (Figure 3A). However, treatment with candesartan-7H (20 mg/kg per day) did not prevent the increase in heart:body weight ratio (Figure 3B), progression of chamber dilatation, contractile dysfunction (Figure 3C), interstitial fibrosis (Figure 3D), or the increase in mRNA levels of fetal cardiac genes and extracellular matrix genes in AT_1Tg-AgtKO mice. Tail-cuff measurements revealed that treatment with candesartan cilexetil and candesartan-7H did not change systolic BP in AT_1Tg-AgtKO mice (Figure S2)

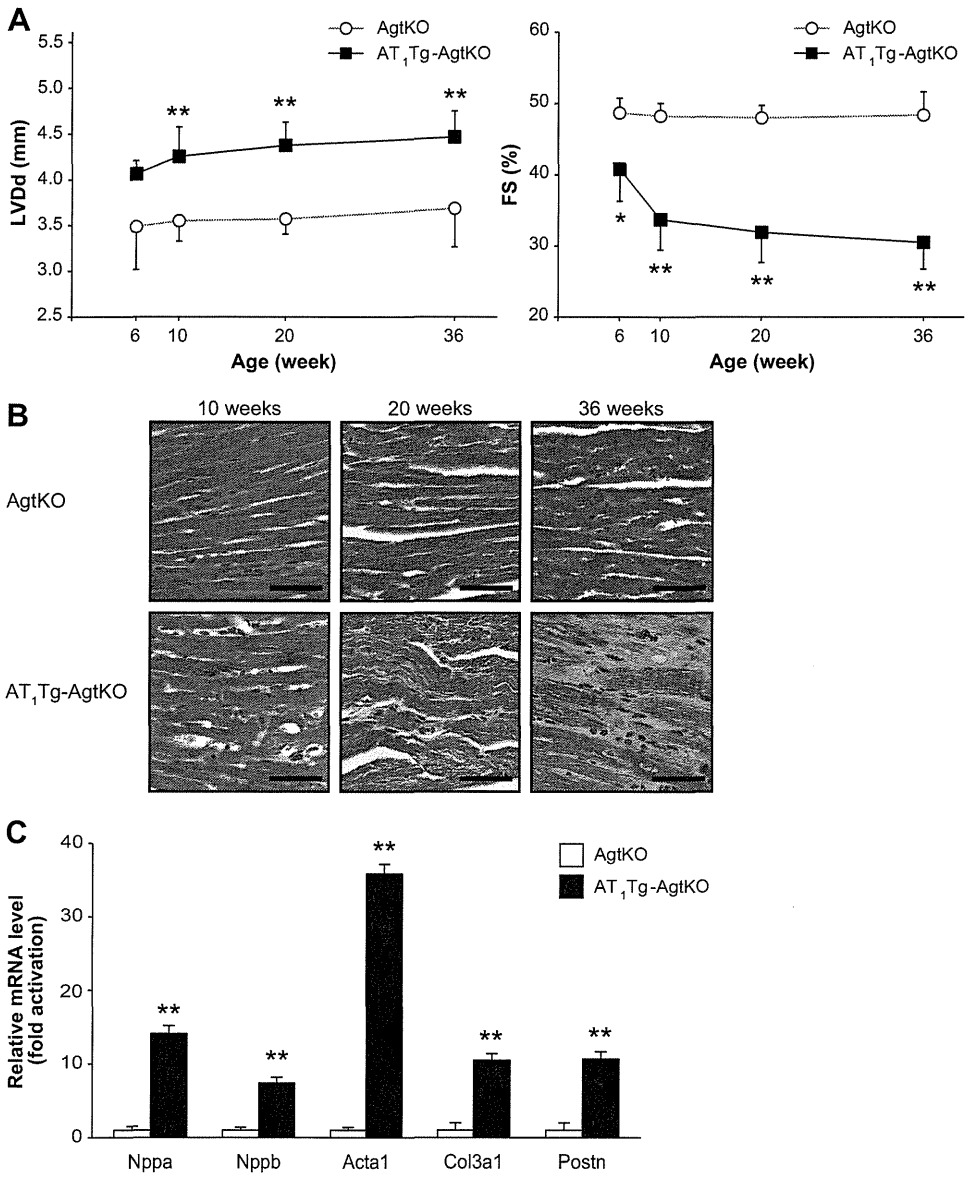

Figure 2. Spontaneous development of cardiac remodeling in angiotensin II type 1 (AT_1) transgenic (AT_1Tg)-angiotensinogen-knockout (AgtKO) mice. **A**, Left ventricular end-diastolic dimension (LVDd) and fractional shortening (FS) of AgtKO (n=7–9) and AT_1Tg-AgtKO (n=9–11) mice measured by echocardiogram at 6, 10, 20, and 36 weeks of age. Data are presented as mean±SEM. *P<0.05, **P<0.01 vs AgtKO mice. ○, AgtKO; ■, AT_1Tg-AgtKO. **B**, Histological sections with Masson trichrome staining of AgtKO and AT_1Tg-AgtKO hearts at 10, 20, and 36 weeks of age. Scale bars, 50 μm. **C**, The mRNA expressions of cardiac genes *Nppa*, *Nppb*, and *Acta1*, and extracellular matrix genes *Col3a1* and *Postn* in AgtKO (n=9) and AT_1Tg-AgtKO (n=9) hearts at 10 weeks of age. □, AgtKO; ■, AT_1Tg-AgtKO. Data are presented as mean±SEM. **P<0.01 vs AgtKO mice.

because Ang II is not produced in AT_1Tg-AgtKO mice. Collectively, these results suggest that cardiac remodeling in AT_1Tg-AgtKO mice was prevented by candesartan, an inverse agonist for the AT_1 receptor, but not by candesartan-7H, which cannot inhibit Ang II–independent AT_1 receptor activation because of a lack of inverse agonist activity.

Discussion

In several GPCRs, the constitutive activity is closely related to physiological function. For example, constitutive activity of the histamine H_3 receptor controls histaminergic neuron activity in rodents.[18] The melanocortin-4 receptor and growth hormone secretagogue receptor have high constitutive activity, and loss of constitutive activity in mutant melanocortin-4 receptors or growth hormone secretagogue receptors leads to obesity or short stature in humans, respectively.[19,20] In contrast, constitutively active mutations in several GPCRs give rise to diseases in humans. For example, somatic mutations of thyrotropin-stimulating hormone receptor or luteinizing hormone receptor lead to hyperfunctioning thyroid adenoma or male precocious puberty, respectively.[21,22]

In the present work, we provide experimental evidence that transgenic myocardial overexpression of the wild-type AT_1 receptor increases constitutive activity of the receptor, leading to cardiac enlargement, interstitial fibrosis, and contractile dysfunction, even in the absence of Ang II. To exclude a

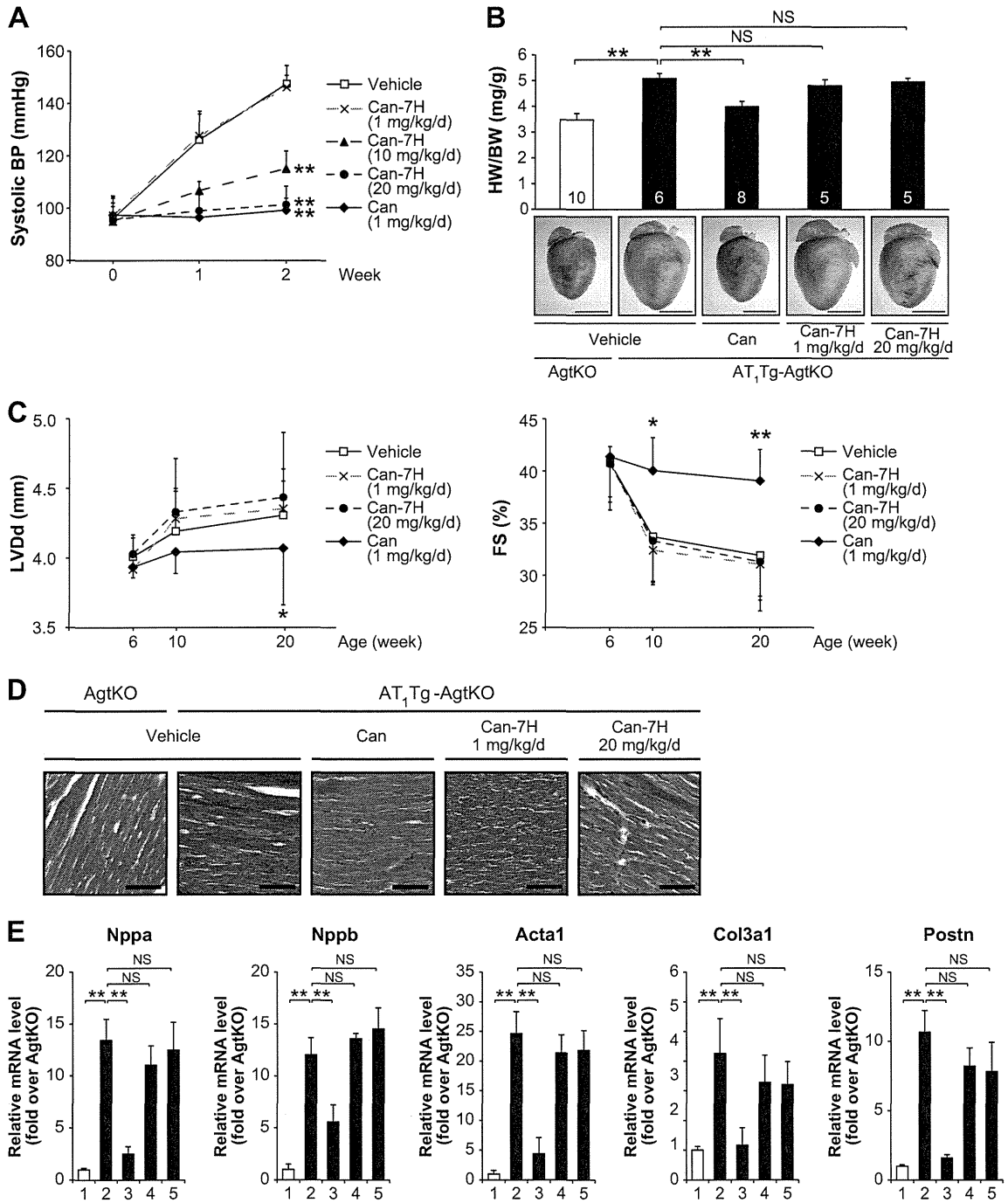

Figure 3. Prevention of cardiac remodeling in angiotensin II (Ang II) type 1 (AT_1) transgenic (AT_1Tg)-angiotensinogen-knockout (AgtKO) mice by candesartan but not by candesartan-7H. **A**, Blood pressure–lowering effects of candesartan cilexetil (Can) and candesartan-7H (Can-7H) in Ang II–infused mice. Eight-week–old C57BL/6J male mice were continuously infused with Ang II (0.6 mg/kg per day) and treated with candesartan cilexetil (1 mg/kg per day), candesartan-7H (1, 10, and 20 mg/kg per day), or vehicle in drinking water (n=5, in each group). *P<0.05, **P<0.01 vs vehicle-treated group. **B**, Heart:body weight ratios and gross hearts in AgtKO and AT_1Tg-Agt KO mice (20 weeks of age) treated with Can (1 mg/kg per day), Can-7H (1, 20 mg/kg per day), or vehicle. Data are presented as mean±SEM. Number of mice for each experiment is indicated in the bars. **P<0.01. Scale bars, 5 mm. **C**, Left ventricular end-diastolic dimension (LVDd) and fractional shortening (FS) of AT_1Tg-AgtKO mice treated with Can or Can-7H. Can (1 mg/kg per day, n=11), Can-7H (1, 20 mg/kg per day; n=7 in each group), or vehicle (n=7) was given for 14 weeks in 6-week–old AT_1Tg-AgtKO mice. Data are presented as mean±SEM. *P<0.05, **P<0.01 vs vehicle-treated group. **D**, Histological sections with Masson trichrome staining in AgtKO and AT_1Tg-Agt KO mice (20 weeks of age) treated with Can (1 mg/kg per day), Can-7H (1, 20 mg/kg per day), or vehicle. Scale bars, 50 μm. **E**, The mRNA expressions of cardiac genes *Nppa*, *Nppb*, and *Acta1* and extracellular matrix genes *Col3a1* and *Postn* in AgtKO (lane 1) and AT_1Tg-Agt KO mice (20 weeks of age) treated with Can (1 mg/kg per day; lane 3), Can-7H (1, 20 mg/kg per day; lane 4, 5, respectively), or vehicle (lane 2). Data are presented as mean±SEM. **P<0.01 vs AgtKO mice. NS indicates not significant (P>0.05). □, vehicle; ×, Can-7H (1 mg/kg per d); ▲, Can-7H (10 mg/kg per d); ●, Can-7H (20 mg/kg per d); ♦, Can (1 mg/kg per d).

contribution of endogenous Ang II to the activity of AT_1 receptor in native tissues, we used AgtKO mice, deficient in the production of Ang II.[13] Furthermore, AT_1Tg-AgtKO mice developed cardiac remodeling regardless of whether they were the offspring of $Agt^{+/-}$ females or $Agt^{-/-}$ females (Figure S3), suggesting that maternal or placental angiotensinogen had little influence on the postnatal development of cardiac remodeling in AT_1Tg-AgtKO mice. Among the renin-angiotensin system components, the mRNA level of the AT_2 receptor was significantly upregulated in AT_1Tg-AgtKO hearts compared with AgtKO hearts (Figure S1A), but the protein level of the AT_2 receptor was comparable between AT_1Tg-AgtKO and AgtKO hearts. Therefore, we believe that constitutive activity of the AT_1 receptor is sufficient for inducing structural and functional cardiac remodeling, when the AT_1 receptor is upregulated in the hearts.

Redistribution of $G\alpha_{q11}$ into the cytosolic fraction in AT_1Tg-AgtKO hearts (Figure 1A) indicates that constitutive activity of the AT_1 receptor is mediated through the $G\alpha_{q11}$-dependent signaling pathway. On binding to Ang II, the AT_1 receptor is phosphorylated by GPCR kinases and recruits β-arrestins, leading to clathrin-coated, pit-dependent internalization and then recycling to the plasma membrane.[23] It has been reported that constitutively active mutant AT_1 receptors are constitutively internalized and recycled when overexpressed in HEK293 cells.[24] In contrast, we showed previously, by immunofluorescence analysis, that the wild-type AT_1 receptor was predominantly localized in the plasma membrane of HEK293 cells expressing the AT_1 receptor.[1] In addition, the expression levels of GPCR kinase 2 and β-arrestins in the particulate fraction relative to the cytosolic fraction were comparable between AT_1Tg-AgtKO and AgtKO hearts (Figure S4). Therefore, we suppose that, in the absence of Ang II, wild-type AT_1 receptor stochastically undergoes subtle and transient conformational changes, leading to partial activation of $G\alpha_{q11}$-depentent signaling without inducing detectable receptor internalization. The AT_1 receptor can also stimulate G protein–independent diverse signaling pathways involving β-arrestins, tyrosine kinases, reactive oxygen species, and AT_1 receptor–associated proteins.[15] Further structure-function analysis will be needed to elucidate the full breadth of the molecular mechanisms and signal transduction network that mediate agonist-independent AT_1 receptor activation in the hearts.

It has been reported that the AT_1 receptor is upregulated in stressed hearts of spontaneously hypertensive rats,[25] 2-kidney 1-clip renovascular hypertensive rats,[25] Tsukuba hypertensive mice,[26] and rats with myocardial infarction.[27] Furthermore, we observed that cardiac expression of the AT_1 receptor was increased ≈8-fold in pressure-overloaded mice after transverse aortic constriction (B_{max}: 142.9±36.5 fmol/mg; n=3) compared with sham-operated mice (B_{max}: 16.4±4.9 fmol/mg; n=3). In addition, it has been reported that the AT_1 receptor is upregulated in response to low-density lipoprotein cholesterol,[28] insulin,[29] glucose,[30] progesterone,[31] and inflammatory cytokines, such as interleukin 1α or interleukin 6,[32,33] in vascular cells. Therefore, it seems quite reasonable to assume that enhancement of constitutive activity of the AT_1 receptor through upregulation of receptor expression may accelerate the progression of atherosclerosis in patients with hypercholesterolemia or diabetes mellitus, especially after menopause. Further studies in animal models will be required to clarify the roles of constitutive activity of the AT_1 receptor in the pathogenesis of cardiovascular and metabolic disorders.

We also demonstrate that treatment with candesartan, inverse agonist for the AT_1 receptor, effectively prevents cardiac remodeling in AT_1Tg-AgtKO mice. The inverse agonist activity of ARBs may provide clinical advantage of inhibiting both Ang II–dependent and -independent receptor activation and, thus, be an important pharmacological parameter defining the beneficial effects on organ protection.[3] Several ARBs are currently available for the treatment of hypertension and heart failure with reduced left ventricular ejection fraction, and their potency of inverse agonist activity differs according to the distinct chemical structure of the drug.[3] For example, the inhibitory effect of olmesartan on both constitutive activity and stretch-induced activation of the AT_1 receptor was significantly higher than that of losartan.[2] According to a recent article,[34] the use of candesartan was associated with lower all-cause mortality than the use with losartan in a Swedish registry of patients with heart failure. Although EXP3174, an active metabolite of losartan, can act as an inverse agonist,[8] it is tempting to speculate that the potent inverse agonist activity of candesartan may explain some of its association with lower mortality in patients with heart failure.

Perspectives

Blockade of the renin-angiotensin system has been shown to be beneficial in patients with hypertension, especially those with cardiovascular and metabolic complications. Our findings show that constitutive activity of the AT_1 receptor contributes to the progression of cardiac remodeling even in the absence of Ang II, when the AT_1 receptor is upregulated in the heart. Inverse agonism of ARBs provides therapeutic effects in the prevention of cardiac remodeling induced by constitutive activity of AT_1 receptor and, thus, has potential impact on long-term outcomes in patients with hypertension. Our work is the first proof-of-principle experiment, to our knowledge, on the in vivo importance of constitutive activity of a native GPCR in the pathogenesis of diseases. Beyond in vitro pharmacological tools, inverse agonists emerge as promising pharmacological candidates in treating diseases caused by enhancement of constitutive activity through upregulation of GPCRs.

Acknowledgments

We thank Drs Sin-ichiro Miura (Fukuoka University) and Motohiro Nishida (Kyushu University) for technical advice and Akane Furuyama, Megumi Ikeda, Yuko Ohtsuki, and Ikuko Sakamoto for their excellent technical assistance.

Sources of Funding

This work was supported in part by grants from Japan Society for the Promotion of Science (KAKENHI 20390218, 21229010, and 23390213; to I.K. and H.A.), Health and Labor Sciences Research grants, Kowa Life Science Foundation, Takeda Science Foundation, Astellas Foundation for Research on Metabolic Disorders, the Uehara Memorial Foundation, the Ichiro Kanehara Foundation,

Mochida Memorial Foundation for Medical and Pharmaceutical Research, and Suzuken Memorial Foundation (to H.A.).

Disclosures

None.

References

1. Yasuda N, Miura S, Akazawa H, Tanaka T, Qin Y, Kiya Y, Imaizumi S, Fujino M, Ito K, Zou Y, Fukuhara S, Kunimoto S, Fukuzaki K, Sato T, Ge J, Mochizuki N, Nakaya H, Saku K, Komuro I. Conformational switch of angiotensin II type 1 receptor underlying mechanical stress-induced activation. *EMBO Rep.* 2008;9:179–186.
2. Qin Y, Yasuda N, Akazawa H, Ito K, Kudo Y, Liao CH, Yamamoto R, Miura S, Saku K, Komuro I. Multivalent ligand-receptor interactions elicit inverse agonist activity of AT(1) receptor blockers against stretch-induced AT(1) receptor activation. *Hypertens Res.* 2009;32:875–883.
3. Akazawa H, Yasuda N, Komuro I. Mechanisms and functions of agonist-independent activation in the angiotensin II type 1 receptor. *Mol Cell Endocrinol.* 2009;302:140–147.
4. Milligan G. Constitutive activity and inverse agonists of G protein-coupled receptors: a current perspective. *Mol Pharmacol.* 2003;64: 1271–1276.
5. Zou Y, Akazawa H, Qin Y, Sano M, Takano H, Minamino T, Makita N, Iwanaga K, Zhu W, Kudoh S, Toko H, Tamura K, Kihara M, Nagai T, Fukamizu A, Umemura S, Iiri T, Fujita T, Komuro I. Mechanical stress activates angiotensin II type 1 receptor without the involvement of angiotensin II. *Nat Cell Biol.* 2004;6:499–506.
6. Mederos y Schnitzler M, Storch U, Meibers S, Nurwakagari P, Breit A, Essin K, Gollasch M, Gudermann T. Gq-coupled receptors as mechano-sensors mediating myogenic vasoconstriction. *EMBO J.* 2008;27: 3092–3103.
7. Rakesh K, Yoo B, Kim IM, Salazar N, Kim KS, Rockman HA. β-Arrestin-biased agonism of the angiotensin receptor induced by mechanical stress. *Sci Signal.* 2010;3:ra46.
8. Miura S, Fujino M, Hanzawa H, Kiya Y, Imaizumi S, Matsuo Y, Tomita S, Uehara Y, Karnik SS, Yanagisawa H, Koike H, Komuro I, Saku K. Molecular mechanism underlying inverse agonist of angiotensin II type 1 receptor. *J Biol Chem.* 2006;281:19288–19295.
9. Sachse R, Shao XJ, Rico A, Finckh U, Rolfs A, Reincke M, Hensen J. Absence of angiotensin II type 1 receptor gene mutations in human adrenal tumors. *Eur J Endocrinol.* 1997;137:262–266.
10. Davies E, Bonnardeaux A, Plouin PF, Corvol P, Clauser E. Somatic mutations of the angiotensin II (AT1) receptor gene are not present in aldosterone-producing adenoma. *J Clin Endocrinol Metab.* 1997;82: 611–615.
11. Billet S, Bardin S, Verp S, Baudrie V, Michaud A, Conchon S, Muffat-Joly M, Escoubet B, Souil E, Hamard G, Bernstein KE, Gasc JM, Elghozi JL, Corvol P, Clauser E. Gain-of-function mutant of angiotensin II receptor, type 1A, causes hypertension and cardiovascular fibrosis in mice. *J Clin Invest.* 2007;117:1914–1925.
12. Paradis P, Dali-Youcef N, Paradis FW, Thibault G, Nemer M. Overexpression of angiotensin II type I receptor in cardiomyocytes induces cardiac hypertrophy and remodeling. *Proc Natl Acad Sci U S A.* 2000; 97:931–936.
13. Tanimoto K, Sugiyama F, Goto Y, Ishida J, Takimoto E, Yagami K, Fukamizu A, Murakami K. Angiotensinogen-deficient mice with hypotension. *J Biol Chem.* 1994;269:31334–31337.
14. Miura S, Feng YH, Husain A, Karnik SS. Role of aromaticity of agonist switches of angiotensin II in the activation of the AT1 receptor. *J Biol Chem.* 1999;274:7103–7110.
15. Hunyady L, Catt KJ. Pleiotropic AT1 receptor signaling pathways mediating physiological and pathogenic actions of angiotensin II. *Mol Endocrinol.* 2006;20:953–970.
16. Zhai P, Galeotti J, Liu J, Holle E, Yu X, Wagner T, Sadoshima J. An angiotensin II type 1 receptor mutant lacking epidermal growth factor receptor transactivation does not induce angiotensin II-mediated cardiac hypertrophy. *Circ Res.* 2006;99:528–536.
17. Shibouta Y, Inada Y, Ojima M, Wada T, Noda M, Sanada T, Kubo K, Kohara Y, Naka T, Nishikawa K. Pharmacological profile of a highly potent and long-acting angiotensin II receptor antagonist, 2-ethoxy-1-[[2′-(1H-tetrazol-5-yl)biphenyl-4- yl]methyl]-1H-benzimidazole-7-carboxylic acid (CV-11974), and its prodrug, (+/−)-1-(cyclohexyloxycarbonyloxy)-ethyl 2-ethoxy-1-[[2′-(1H-tetrazol-5- yl)biphenyl-4-yl]methyl]-1H-benzimidazole-7-carboxylate (TCV-116). *J Pharmacol Exp Ther.* 1993;266:114–120.
18. Morisset S, Rouleau A, Ligneau X, Gbahou F, Tardivel-Lacombe J, Stark H, Schunack W, Ganellin CR, Schwartz JC, Arrang JM. High constitutive activity of native H3 receptors regulates histamine neurons in brain. *Nature.* 2000;408:860–864.
19. Srinivasan S, Lubrano-Berthelier C, Govaerts C, Picard F, Santiago P, Conklin BR, Vaisse C. Constitutive activity of the melanocortin-4 receptor is maintained by its N-terminal domain and plays a role in energy homeostasis in humans. *J Clin Invest.* 2004;114:1158–1164.
20. Pantel J, Legendre M, Cabrol S, Hilal L, Hajaji Y, Morisset S, Nivot S, Vie-Luton MP, Grouselle D, de Kerdanet M, Kadiri A, Epelbaum J, Le Bouc Y, Amselem S. Loss of constitutive activity of the growth hormone secretagogue receptor in familial short stature. *J Clin Invest.* 2006;116: 760–768.
21. Parma J, Duprez L, Van Sande J, Cochaux P, Gervy C, Mockel J, Dumont J, Vassart G. Somatic mutations in the thyrotropin receptor gene cause hyperfunctioning thyroid adenomas. *Nature.* 1993;365:649–651.
22. Shenker A, Laue L, Kosugi S, Merendino JJ Jr, Minegishi T, Cutler GB Jr. A constitutively activating mutation of the luteinizing hormone receptor in familial male precocious puberty. *Nature.* 1993;365:652–654.
23. Shenoy SK, Lefkowitz RJ. Angiotensin II-stimulated signaling through G proteins and β-arrestin. *Sci STKE.* 2005;2005:cm14.
24. Miserey-Lenkei S, Parnot C, Bardin S, Corvol P, Clauser E. Constitutive internalization of constitutively active agiotensin II AT(1A) receptor mutants is blocked by inverse agonists. *J Biol Chem.* 2002;277: 5891–5901.
25. Suzuki J, Matsubara H, Urakami M, Inada M. Rat angiotensin II (type 1A) receptor mRNA regulation and subtype expression in myocardial growth and hypertrophy. *Circ Res.* 1993;73:439–447.
26. Fujii N, Tanaka M, Ohnishi J, Yukawa K, Takimoto E, Shimada S, Naruse M, Sugiyama F, Yagami K, Murakami K, Miyazaki H. Alterations of angiotensin II receptor contents in hypertrophied hearts. *Biochem Biophys Res Commun.* 1995;212:326–333.
27. Nio Y, Matsubara H, Murasawa S, Kanasaki M, Inada M. Regulation of gene transcription of angiotensin II receptor subtypes in myocardial infarction. *J Clin Invest.* 1995;95:46–54.
28. Nickenig G, Jung O, Strehlow K, Zolk O, Linz W, Scholkens BA, Bohm M. Hypercholesterolemia is associated with enhanced angiotensin AT1-receptor expression. *Am J Physiol.* 1997;272:H2701–H2707.
29. Nickenig G, Roling J, Strehlow K, Schnabel P, Bohm M. Insulin induces upregulation of vascular AT1 receptor gene expression by posttranscriptional mechanisms. *Circulation.* 1998;98:2453–2460.
30. Sodhi CP, Kanwar YS, Sahai A. Hypoxia and high glucose upregulate AT1 receptor expression and potentiate ANG II-induced proliferation in VSM cells. *Am J Physiol Heart Circ Physiol.* 2003;284:H846–H852.
31. Nickenig G, Strehlow K, Wassmann S, Baumer AT, Albory K, Sauer H, Bohm M. Differential effects of estrogen and progesterone on AT(1) receptor gene expression in vascular smooth muscle cells. *Circulation.* 2000;102:1828–1833.
32. Wassmann S, Stumpf M, Strehlow K, Schmid A, Schieffer B, Bohm M, Nickenig G. Interleukin-6 induces oxidative stress and endothelial dysfunction by overexpression of the angiotensin II type 1 receptor. *Circ Res.* 2004;94:534–541.
33. Sasamura H, Nakazato Y, Hayashida T, Kitamura Y, Hayashi M, Saruta T. Regulation of vascular type 1 angiotensin receptors by cytokines. *Hypertension.* 1997;30:35–41.
34. Eklind-Cervenka M, Benson L, Dahlstrom U, Edner M, Rosenqvist M, Lund LH. Association of candesartan vs losartan with all-cause mortality in patients with heart failure. *JAMA.* 2011;305:175–182.

Journal of Molecular and Cellular Cardiology xxx (2012) xxx–xxx

Contents lists available at SciVerse ScienceDirect

Journal of Molecular and Cellular Cardiology

journal homepage: www.elsevier.com/locate/yjmcc

Original article

Role of regulatory T cells in atheroprotective effects of granulocyte colony-stimulating factor

Raita Uchiyama [a,1], Hiroshi Hasegawa [a,1], Yoshihito Kameda [a], Kazutaka Ueda [a], Yoshio Kobayashi [a], Issei Komuro [b], Hiroyuki Takano [c,*]

[a] Department of Cardiovascular Science and Medicine, Chiba University Graduate School of Medicine, 1-8-1 Inohana, Chuo-ku, Chiba 260-8670, Japan
[b] Department of Cardiovascular Medicine, Osaka University Graduate School of Medicine, 2-2 Yamadaoka, Suita, Osaka 565-0871, Japan
[c] Department of Molecular Cardiovascular Pharmacology, Chiba University Graduate School of Pharmaceutical Sciences, 1-8-1 Inohana, Chuo-ku, Chiba 260-8675, Japan

ARTICLE INFO

Article history:
Received 9 September 2011
Received in revised form 7 December 2011
Accepted 29 December 2011
Available online xxxx

Keywords:
Atherosclerosis
Regulatory T cells
G-CSF
Cytokine
Foxp3

ABSTRACT

We and others have previously reported that granulocyte colony-stimulating factor (G-CSF) prevents left ventricular remodeling and dysfunction after myocardial infarction in animal models and human. We have also reported that G-CSF inhibits the progression of atherosclerosis in animal models, but its precise mechanism is still elusive. So, we examined the effects of G-CSF on atherosclerosis in apolipoprotein E-deficient ($ApoE^{-/-}$) mice. Twelve-week-old male $ApoE^{-/-}$ mice were subcutaneously administrated with 200 μg/kg of G-CSF or saline once a day for 5 consecutive days per a week for 4 weeks. Atherosclerotic lesion of aortic sinus was significantly reduced in the G-CSF-treated mice compared with the saline-treated mice (35% reduction, $P<0.05$). G-CSF significantly reduced the expression level of interferon-γ by 31% and increased the expression level of interleukin-10 by 20% in atherosclerotic lesions of aortic sinus. G-CSF increased the number of $CD4^+CD25^+$ regulatory T cells in lymph nodes and spleen, and enhanced the suppressive function of regulatory T cells *in vitro*. G-CSF markedly increased the number of Foxp3-positive regulatory T cells in atherosclerotic lesions of aortic sinus. Administration of anti-CD25 antibody (PC61) that depletes regulatory T cells abrogated these atheroprotective effects of G-CSF. Moreover, in $ApoE^{-/-}/CD28^{-/-}$ mice, that lack regulatory T cells, the protective effects of G-CSF on atherosclerosis were not recognized. These findings suggest that regulatory T cells play an important role in the atheroprotective effects of G-CSF.

1. Introduction

Atherosclerosis is a progressive disease characterized by the accumulation of lipids and fibrous elements in arterial walls. Over the past two decades, an understanding of the importance of inflammation in the initiation and progression of atherosclerosis has greatly increased. Under normal conditions, the endothelial cells of the arterial wall resist adhesion and aggregation of leukocytes and promote fibrinolysis. When activated by stimuli such as hypertension, smoking, insulin resistance or inflammation, the endothelial cells express a series of adhesion molecules that selectively recruit various classes of leukocytes. Blood monocytes, which are the most numerous inflammatory cells within the atherosclerotic lesions, adhere to the dysfunctional endothelial surface by binding to leukocyte adhesion molecules [1]. Helper T cells and the associated cytokines have been reported to play a crucial role in the pathophysiology of atherosclerosis. $CD4^+CD25^+$ regulatory T cells (Tregs) subset constitutes 5–10% of all peripheral $CD4^+$ T cell population and are specialized for the suppressions of both type 1 helper T (Th1) and type 2 helper T (Th2) immune responses [2]. Tregs, as dedicated suppressors of diverse immune responses and important gatekeepers of immune homeostasis, contribute to the maintenance of the peripheral tolerance. Recently, it was reported that Tregs prevent the progression of atherosclerosis and a defect in Tregs favors atherogenesis [3–5].

Granulocyte colony-stimulating factor (G-CSF) is a member of a group of glycoproteins called hematopoietic cytokines. G-CSF induces the release of hematopoietic stem cells and endothelial progenitor cells from bone marrow into the peripheral blood circulation [6]. Moreover, G-CSF has been reported to modulate immune system and ameliorate immune-mediated diseases of animals [7]. We and others have previously reported that G-CSF prevents left ventricular remodeling and dysfunction after myocardial infarction (MI) in animal models and human [8–12]. G-CSF activates multiple signaling pathways such as Akt and Janus family kinase-2 and signal transducer and activation of transcription-3 (Jak2-STAT3) pathway in cardiac myocytes. G-CSF decreases cardiomyocyte death and increases the number of blood vessels, suggesting the importance of direct actions of G-CSF on the myocardium rather than through mobilization and differentiation of

* Corresponding author at: Department of Molecular Cardiovascular Pharmacology, Chiba University Graduate School of Pharmaceutical Sciences, 1-8-1 Inohana, Chuo-ku, Chiba 260-8675, Japan. Tel./fax: +81 43 226 2883
E-mail address: htakano-cib@umin.ac.jp (H. Takano).
[1] These authors contributed equally to this work.

0022-2828/$ – see front matter © 2012 Elsevier Ltd. All rights reserved.
doi:10.1016/j.yjmcc.2011.12.016

stem cells. We and others also reported that G-CSF prevents the progression of atherosclerosis [13–16]. G-CSF significantly reduced the stenosis score of coronary artery and lipid plaque area of thoracic aorta in the myocardial infarction-prone Watanabe heritable hyperlipidemic (WHHL-MI) rabbits and prevented an increase in neointima/media ratio in the vascular injury model of rabbit [13]. However, its precise mechanism of G-CSF on atherosclerosis has been still elusive. In human and animal studies, G-CSF stimulation alters the T cell function and modulates the balance between Th1 and Th2 immune responses by affecting cytokine production [17]. G-CSF stimulation reduces cytotoxic activity and proliferative response of human and murine T cells [18]. Recently, G-CSF was reported to prevent autoimmune type 1 diabetes, graft-versus-host disease and transplanted heart allograft acceptability through enhancement of $CD4^+CD25^+$ Tregs subset [19,20]. Therefore, the aim of this study was to elucidate whether Tregs subset is involved in the atheroprotective mechanism of G-CSF.

2. Materials and methods

2.1. Animal model of atherosclerosis

Apolipoprotein E-deficient ($ApoE^{-/-}$) mice were purchased from the Jackson Laboratory (Bar Harbor, ME). Twelve-week-old male $ApoE^{-/-}$ mice were fed with a proatherogenic diet (1.25% cholesterol, 7.5% cocoa butter, 7.5% casein, 0.5% sodium cholate) (Oriental Yeast Co., Tokyo, Japan) ad libitum for 28 days [21]. These animals were then divided into 2 groups: saline group that received saline and G-CSF group that received G-CSF (rhG-CSF, Kirin Brewery Co., Ltd., Tokyo, Japan). Mice were subcutaneously administrated with 200 μg/kg of G-CSF or same volume (100 μl) of saline once a day for 5 consecutive days per a week for 4 weeks. After 28 days of G-CSF or saline treatment, mice were sacrificed and analyzed.

To deplete Tregs, twelve-week-old male $ApoE^{-/-}$ mice were intraperitoneally injected 100 μg of purified anti-mouse CD25 antibody (clone PC61; Biolegend, San Diego, CA) at day 0 and day 14. These Tregs-depleted mice started proatherogenic diet and each treatment from day 0. At 28 days after first injection, mice were sacrificed and analyzed. To determine the role of Tregs in the mechanisms of G-CSF-induced atheroprotective effect, we used $CD28^{-/-}$ mice. The construction and characterization of $CD28^{-/-}$ mice has been described previously [22]. $ApoE^{-/-}$ mice were crossed with $CD28^{-/-}$ mice and the heterozygous progeny were intercrossed to generate $ApoE^{-/-}$/$CD28^{-/-}$ double knockout (DKO) mice. Animal genotype was identified by a polymerase chain reaction (PCR)-based assay. All protocols were approved by the Institutional Animal Care and Use Committee of Chiba University.

2.2. Atherosclerotic lesion assessment at aortic sinus

After overnight fasting, blood was collected by the cardiac puncture under anesthetic condition using pentobarbital sodium (60 mg/kg intraperitoneal injection). Serum total cholesterol and high-density lipoprotein cholesterol levels were determined by high-performance liquid chromatography at SRL (Tokyo, Japan).

The aorta was perfused *in situ* with phosphate buffered saline (PBS), and the heart was removed and the proximal aorta containing the aortic sinus was embedded in OCT compounds (Tissue-Tek, CA). Five sections (10 μm thickness) of the aortic sinus were collected from each mouse and stained with Oil Red-O (Sigma-Aldrich, St Louis, MO) as described previously [21]. For the quantitative analysis of the area of atherosclerosis, section images were captured digitally (Axio Vision, Zeiss, Germany) and the average lesion areas of five separate sections from each mouse were obtained with Image J 1.38 (National Institutes of Health, MD).

2.3. Immunohistochemistry

Immunohistochemical staining with CD3ε (Santa Cruz Biotechnology, Santa Cruz, CA), MOMA-2 (BMA Biomedicals AG, Switzerland), IFN-γ (Biosource International, Camarillo, CA), interleukin-10 (IL-10) (Santa Cruz Biotechnology) and Foxp3 (FJK-16 s, eBioscience, San Diego, CA) of atherosclerotic lesions at the aortic sinus were performed. Quantitative analysis of MOMA-2, IFN-γ and IL-10-immunostaining were evaluated as a ratio of the positive-stained area to total plaque area in the atherosclerotic lesion. At least three sections per mouse were examined for each immunostaining and appropriate negative controls were used. To evaluate the extent of nonspecific binding in the immunohistochemical experiments, control sections were incubated in the absence of primary antibody. As negative controls of the stainings of IFN-γ and IL-10, aorta of wild type mice were used. To define the subtype of infiltrated macrophages in the atherosclerotic lesions, we analyzed the expression level of CD11c, an M1 macrophage marker [23].

2.4. Quantitative real-time PCR at aortic sinus and whole aorta

At 28 days after first injection, mice were sacrificed under anesthetic condition using pentobarbital sodium (60 mg/kg intraperitoneal injection). The aorta was perfused *in situ* with phosphate buffered saline (PBS), and the whole aorta with aortic sinus was removed. These samples were frozen with liquid nitrogen and stored at −80 °C until each assay. Quantitative real-time PCR (qRT-PCR) analysis for transforming growth factor-β (TGF-β) was performed as described previously [24]. Total RNA was extracted from sample using the RNeasy kit (QIAGEN, Valencia, CA). We used 0.5 μg of total RNA to generate cDNA using the Super Script VILO cDNA synthesis kit (Invitrogen, Carlsbad, CA). qRT-PCR was carried out on a LightCycler system (Roche, Mannheim, Germany) using probes from Universal Probe Library and the TaqMan Master Mix. Sequence of primers and the respective Universal Probe Library probes were as follows: Tgf-beta: forward; CACCATCCATGACATGAACC, reverse; CCGCACACAGCAGTTCTTC; IFN-γ: forward; ATCTGGAGGAACTGGCAAA, reverse; CAAGACTTCAAAGAGTCTGAGGTA; IL-10: forward; CAGAGCCACATGCTCCTAGA, reverse; TGTCCAGCTGGTCCTTTGTT; Gapdh: forward; TGTCCGTCGTGGATCTGAC, reverse; CCTGCTTCACCACCTTCTTG. Relative expression of target genes was calculated with the comparative CT method. Each

Table 1
Body weight and cholesterol levels.

	$ApoE^{-/-}$				DKO	
			PC61			
	saline	G-CSF	saline	G-CSF	saline	G-CSF
Body weight, g	22.7 ± 1.2	22.4 ± 0.8	22.4 ± 0.9	23.6 ± 1.1	24.2 ± 0.6	23.1 ± 0.7
Total cholesterol, mg/dl	3306 ± 171	3527 ± 207	3321 ± 359	3259 ± 245	3767 ± 514	3965 ± 507
HDL cholesterol, mg/dl	29.3 ± 7.3	24.5 ± 4.8	30.8 ± 7.4	28.8 ± 7.5	23.2 ± 6.2	26.2 ± 7.9

HDL indicates high-density lipoprotein. DKO indicates $ApoE^{-/-}$/$CD28^{-/-}$ double knockout mice. $ApoE^{-/-}$ mice and DKO mice were treated by saline or G-CSF for 28 days. The means ± SEM of 10 animals are shown.

Please cite this article as: Uchiyama R, et al, Role of regulatory T cells in atheroprotective effects of granulocyte colony-stimulating factor, J Mol Cell Cardiol (2012), doi:10.1016/j.yjmcc.2011.12.016

sample was run in duplicate, and the results were systematically normalized using Gapdh.

2.5. Mobilization procedure of Tregs and flow cytometry analysis

Twelve-week-old male C57BL/6 mice received G-CSF at a dose of 200 μg of G-CSF or saline once a day for 5 consecutive days per a week for 4 weeks. At day 28, the total cells of spleen and inguinal lymph nodes were taken and the cell surface phenotype of splenocytes and lymphocytes were analyzed by flow cytometry. All cells were incubated in ice cold PBS supplemented with 3% fetal calf serum and 0.1% azide. One million cells per sample were incubated for 15 minutes at ice cold temperature with the following mAbs: Phycoerythrin (PE)-conjugated anti-mouse CD4 (clone L3T4, BD Biosciences, Le Pont de Claix, France), Fluorescein isothiocyanate (FITC)-conjugated anti-mouse CD25 (clone 7D4, BD Biosciences, Le Pont de Claix, France).

At day 28, the total cells of spleen were taken and the cell phenotypes of lymphocytes were analyzed by flow cytometry. After magnetic activated cell sorter (MACS) with $CD4^+$ antibody and the stimulation with phorbol myristate acetate (PMA) and ionomycin, the cells were incubated with permeabilization buffer and stained with FITC-labeled anti-IFN-γ antibody and PE-labeled anti-IL-4 antibody for analysis with a flow cytometer [19]. $CD4^+$IFN-γ^+IL-4^- cells and $CD4^+$IFN-γ^- IL-4^+ cells were defined as Th1 cells and Th2 cells, respectively, and the Th1/Th2 ratio was calculated.

Thirty thousand events were acquired using EPICS ALTRA flow cytometric analysis (Beckman Coulter, Fullerton, CA). Analysis of the acquired data was performed using Expo32 MultiCOMP software (Beckman Coulter, Fullerton, CA).

2.6. Isolation and functional assays of Tregs

Tregs were isolated from spleen cell suspensions by the $CD4^+CD25^+$ regulatory T cell isolation kit (Miltenyi Biotec, Tokyo, Japan), which depletes samples of non-$CD4^+$ T cells followed by positive selection of $CD4^+CD25^+$ cells. The purity of the isolated $CD4^+CD25^+$ cells was

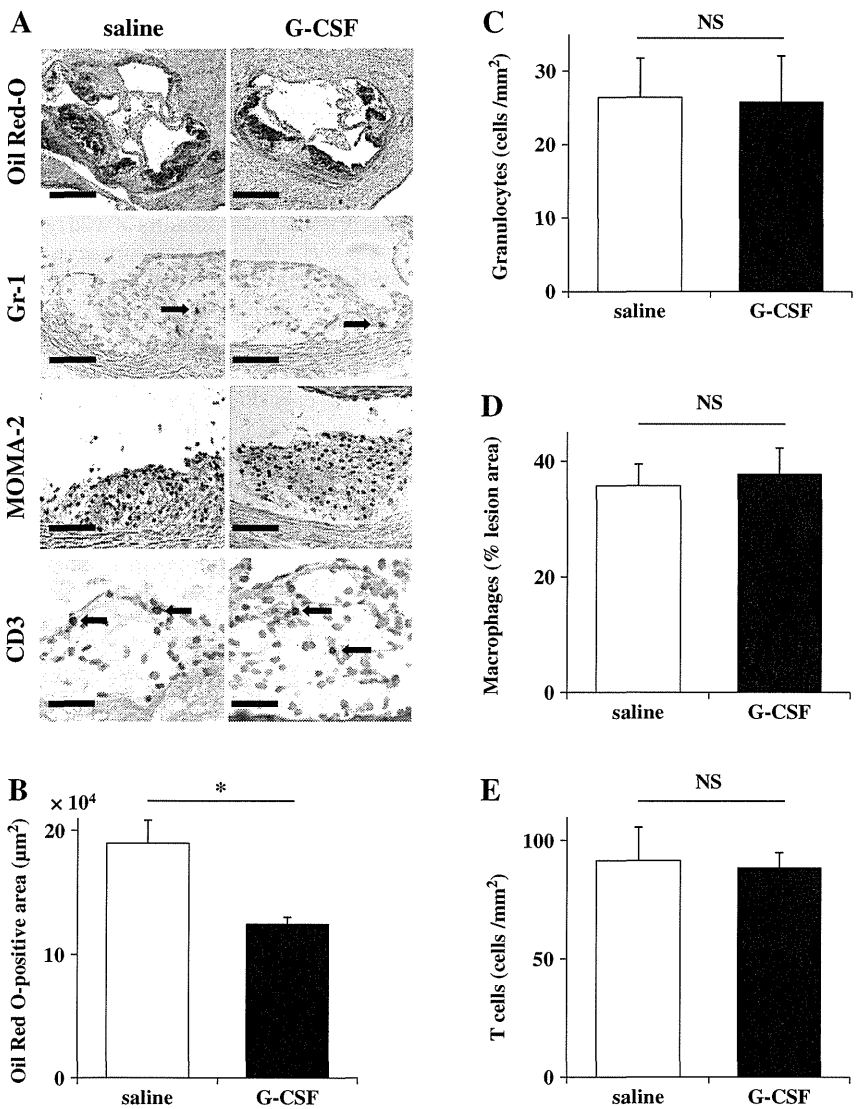

Fig. 1. Effects of G-CSF on atherosclerotic lesions at the aortic sinus in ApoE$^{-/-}$ mice. (A) Representative photographs of atherosclerotic lesion formation (Oil Red-O staining) (Scale bars; 400 μm) and immunostaining of Gr-1 (Scale bars; 100 μm), MOMA-2 (Scale bars; 100 μm) and CD3 (Scale bars; 50 μm) at the aortic sinus of each mouse fed atherogenic diet in the saline group and the G-CSF group. (B) Quantitative analysis of the degree of atherosclerosis at the aortic sinus in both groups. The average lesion area of five sections at the aortic sinus from each mouse was quantified morphometrically as described in Materials and methods. (C) The number of infiltrated granulocytes in the atherosclerotic lesion calculated by immunostaining with Gr-1. (D) The lesion area of infiltrated macrophages in the atherosclerotic lesion calculated by immunostaining with MOMA-2. (E) The number of infiltrated T lymphocyte in the atherosclerotic lesion calculated by immunostaining with CD3. *$P<0.05$. NS indicates that there is no significant difference between the groups. The means ± SEM of 10 animals are shown.

Please cite this article as: Uchiyama R, et al, Role of regulatory T cells in atheroprotective effects of granulocyte colony-stimulating factor, J Mol Cell Cardiol (2012), doi:10.1016/j.yjmcc.2011.12.016

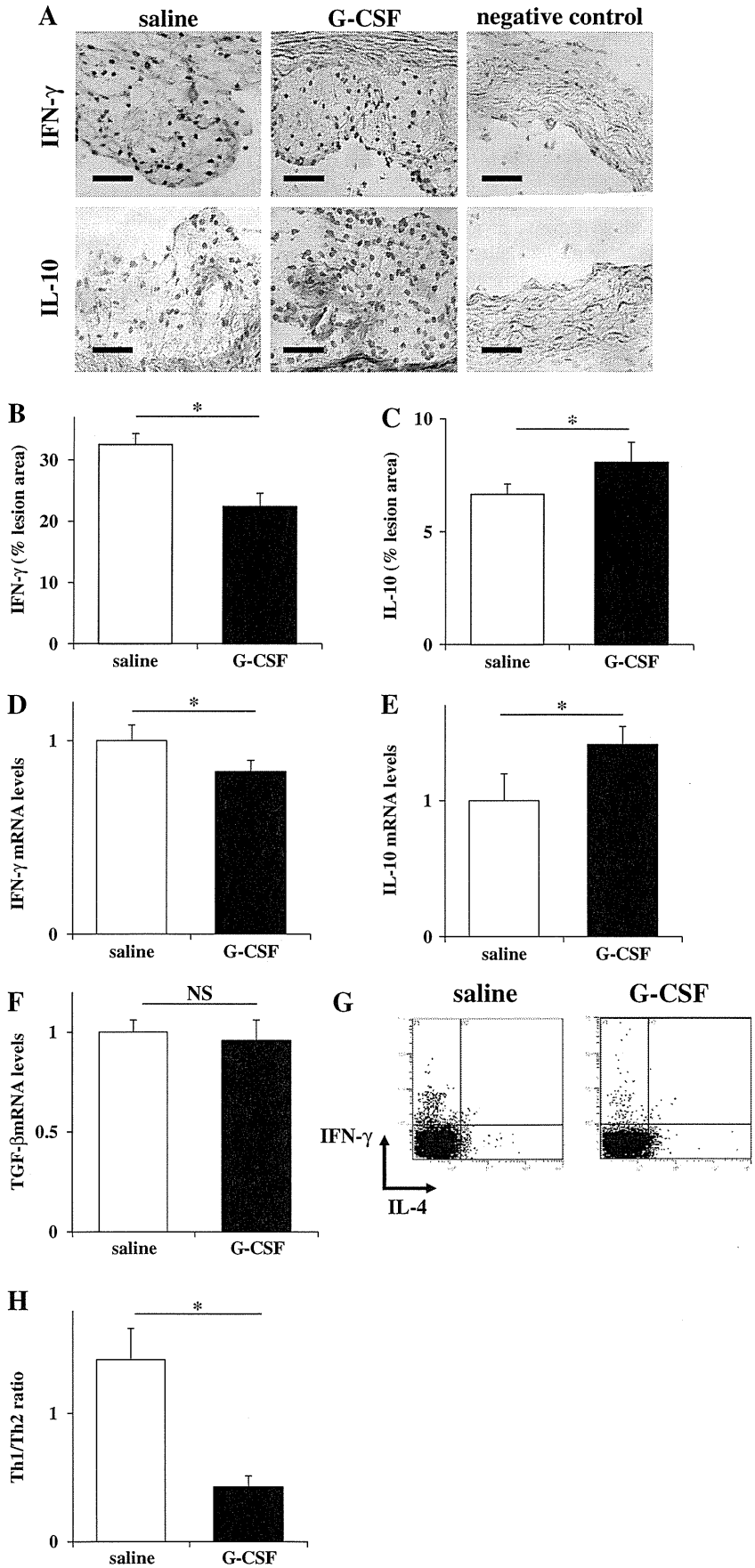
A
saline
G-CSF
negative control
IFN-γ
IL-10
B
IFN-γ (% lesion area)
30
20
10
0
saline
G-CSF
*
C
IL-10 (% lesion area)
10
5
0
saline
G-CSF
*
D
IFN-γ mRNA levels
1
0
saline
G-CSF
*
E
IL-10 mRNA levels
1
0
saline
G-CSF
*
F
TGF-βmRNA levels
1
0.5
0
saline
G-CSF
NS
G
saline
G-CSF
IFN-γ
IL-4
H
Th1/Th2 ratio
1
0
saline
G-CSF
*

>85% by fluorescence-activated cell sorter analysis. All suppression assays were performed in 96-well round-bottom plates in a final volume of 200 μl/well of RPMI 1640 medium (Sigma-Aldrich, St Louis, MO) supplemented with 10% FCS, 10 mmol/l Hepes, 50 μmol/l 2β-mercaptoethanol and antibiotics. Before the assay, 96-well plates were coated with 50 μl of a final concentration of 10 μg/ml anti-CD3 (Cedar-Lane Laboratories, Burlington, NC). The $CD4^+CD25^-$ responder cells were plated at 5×10^4/well alone or in combination with $CD4^+CD25^+$ Tregs at 5×10^4/well and incubated at 37 °C with 5% CO_2 for 72 h. Then 1×10^5 irradiated (3000 rads) splenocytes were added as antigen-presenting cells. Cultures were pulsed with [^{3}H] thymidine for the last 16 h of culture [25]. Cell proliferation was assayed by scintillation counting (β counter). Percent inhibition of proliferation was determined from the following formula: 1 - (median [^{3}H] thymidine uptake of 1:1 $CD4^+CD25^+$:$CD4^+CD25^-$ coculture/median [^{3}H] thymidine uptake of $CD4^+CD25^+$ cells).

2.7. Statistical analysis

Data are presented as mean ± SEM. An unpaired Student *t*-test was used to detect significant differences when two groups were compared. One-way ANOVA was used to compare the differences among four groups with Fisher's PLSD test for post hoc analysis. $P<0.05$ was considered statistically significant.

3. Results

3.1. Atherosclerosis at aortic sinus

There were no significant differences between the saline- and the G-CSF-treatment groups in body weight, serum total cholesterol and high-density lipoprotein cholesterol levels (Table 1). The degree of atherosclerotic legion assessed by Oil Red-O staining at the aortic sinus was significantly reduced in the G-CSF-treated mice compared with the saline-treated mice (G-CSF group: $12.4\pm0.6\times10^4$ μm^2 vs. saline group: $19.0\pm1.9\times10^4$ μm^2, $P<0.05$) (Fig. 1A, B). There was no significant change in the number of infiltrated granulocytes in atherosclerotic lesions between the two groups (G-CSF group: 22.1 ± 18 cells/mm^2 vs. saline group: 23.5 ± 14 cells/mm^2, $P=0.87$) (Fig. 1A, C). Immunohistochemical staining on atherosclerotic lesions of aortic sinus revealed that the percentage of cross-sectional area occupied by macrophages (MOMA-2-positive staining) was not significantly different between the two groups (G-CSF group: 37.7 ± 13% vs. saline group: 35.8 ± 9.9%, $P=0.75$) (Fig. 1A, D). The ratio of CD11c-positive M1 macrophages to total infiltrated cells was not changed in the atherosclerotic lesions of the G-CSF-treated mice compared to the saline-treated mice (G-CSF group: 8.2 ± 1.1% vs. saline group: 9.0 ± 0.5%, $P=0.31$). The number of CD3-positive T cells was not also significantly different between the two groups (G-CSF group: 88.4 ± 19 cells/mm^2 vs. saline group: 91.5 ± 37 cells/mm^2, $P=0.87$) (Fig. 1A, E).

3.2. Effect of G-CSF on cytokine expression

To elucidate the mechanisms by which G-CSF reduced the degree of atherosclerosis, we examined the local cytokine expression in the saline- and the G-CSF-treated mice. Level of proinflammatory cytokine IFN-γ in the atherosclerotic legions was lower in the G-CSF-treated mice compared with the saline-treated mice (G-CSF group: 22.4 ± 2.7% vs. saline group: 32.5 ± 2.2%, $P<0.05$) (Fig. 2A, B). Meanwhile, G-CSF treatment increased the level of antiinflammatory cytokine IL-10 in the atherosclerotic legions (G-CSF group: 8.1 ± 0.9% vs. saline group: 6.7 ± 0.5%, $P<0.05$) (Fig. 2A, C). The expression levels of IFN-γ and IL-10 mRNA were also significantly different between the two groups (IFN-γ; G-CSF group: 0.8 ± 0.1% vs. saline group: 1.0 ± 0.1%, $P<0.05$, IL-10; G-CSF group: 1.4 ± 0.1% vs. saline group: 1.0 ± 0.2%, $P<0.05$) (Fig. 2D, E). Since we could not perform TGF-β immunostaining due to technical problems, we examined the expression level of TGF-β mRNA by using qRT-PCR. The expression level of TGF-β mRNA was not significantly different between the two groups (Fig. 2F).

We examined the effects of G-CSF on Th1/Th2 balance. The Th1/Th2 ratio was significantly reduced in the G-CSF-treated mice (G-CSF group: 0.4 ± 0.1 vs. saline group: 1.4 ± 0.2, $P<0.01$) (Fig. 2G, H).

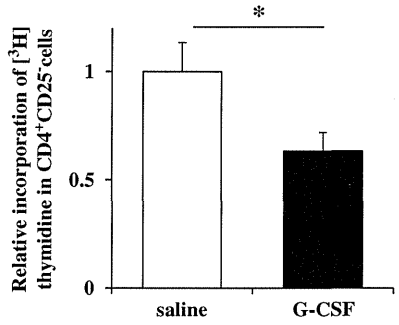

Fig. 3. Effects of G-CSF on the inhibitory function of Tregs. $CD4^+CD25^-$ effector T cells were co-cultured with Tregs from the saline- or the G-CSF-treated mice at the ratio of 1:1 and the incorporation of [^{3}H] thymidine in $CD4^+CD25^-$ cells was counted. *$P<0.05$. The means ± SEM of 6 animals are shown.

3.3. Effect of G-CSF on function of Tregs

To evaluate whether the function of Tregs is influenced by G-CSF treatment, we compared the suppressive function of the Tregs isolated from the saline- and the G-CSF-treated mice. $CD4^+CD25^+$ Tregs from each mouse were co-cultured with $CD4^+CD25^-$ effector cells from wild type mice at the ratio of 1:1 in cell number. Tregs from the G-CSF-treated mice significantly inhibited the incorporation of [^{3}H] thymidine in $CD4^+CD25^-$ effector cells compared with Tregs from the saline-treated mice (Fig. 3).

3.4. Effect of G-CSF on the number of Tregs

To elucidate the mechanism of antiinflammatory effects of G-CSF, we investigated whether G-CSF increases the number of Tregs or not. First of all, we examined the systemic effects of G-CSF on the number of Tregs by flow cytometry analysis of cells from spleen and inguinal lymph nodes of C57BL/6 mice. G-CSF increased the number of $CD4^+CD25^+$ Tregs in spleen (G-CSF group: $249.0\pm18.0\times10^4$ cells vs. saline group: $88.2\pm4.2\times10^4$ cells, $P<0.01$) (Fig. 4A, B) and inguinal lymph nodes (G-CSF group: $54.0\pm5.2\times10^3$ cells vs. saline group: $31.0\pm2.8\times10^3$ cells, $P<0.01$) (Fig. 4A, C).

We next examined whether G-CSF enhances the number of Tregs in atherosclerotic lesions. G-CSF significantly increased the number of Foxp3-positive Tregs in the atherosclerotic legions of aortic sinus (Fig. 5A, B). The number of Foxp3-positive regulatory T cells was 3.1-fold increased at the atherosclerotic lesions of the G-CSF-treated

Fig. 2. Effects of G-CSF on cytokine levels in atherosclerotic lesion at the aortic sinus. (A) Panels are representative photographs of immunostaining with IFN-γ and IL-10 in the atherosclerotic lesion of the G-CSF-treated mice and the saline-treated mice and the aorta of wild type mice (negative control). (B) Levels of IFN-γ calculated in the atherosclerotic legion of the G-CSF-treated mice and the saline-treated mice. (C) Levels of IL-10 calculated in the atherosclerotic legion of the G-CSF-treated mice and the saline-treated mice. (D) Expression levels of IFN-γ mRNA detected by real-time PCR analysis. (E) Expression levels of IL-10 mRNA detected by real-time PCR analysis. (F) Expression levels of TGF-β mRNA detected by real-time PCR analysis. (G) The proportions of $CD4^+$IFN-γ^+IL-4^- cells and $CD4^+$IFN-γ^-IL-4^+ cells from spleen of the G-CSF- and the saline-treated mice assessed by flow cytometric analysis. (H) The Th1/Th2 ratio in spleen of the G-CSF- and the saline-treated mice assessed by flow cytometric analysis. *$P<0.05$. NS indicates that there is no significant difference between the two groups. Scale bars indicates 50 μm. The means ± SEM of 10 animals are shown.

Please cite this article as: Uchiyama R, et al, Role of regulatory T cells in atheroprotective effects of granulocyte colony-stimulating factor, J Mol Cell Cardiol (2012), doi:10.1016/j.yjmcc.2011.12.016

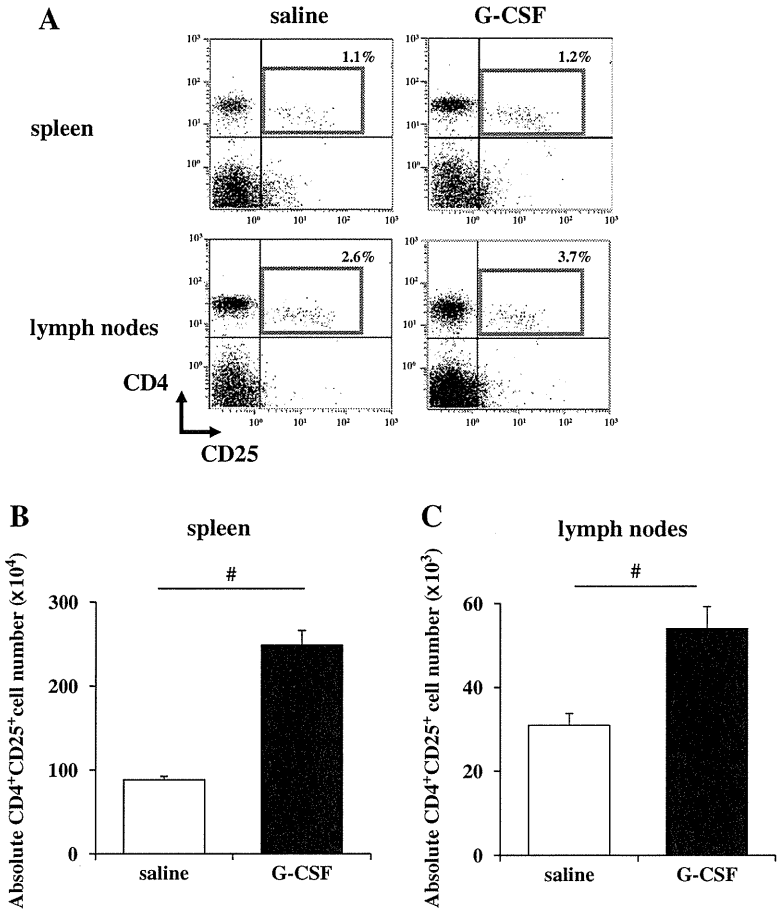

Fig. 4. Effects of G-CSF on the total cell number of Tregs in spleen and inguinal lymph nodes. (A) The proportions of $CD4^+CD25^+$ Tregs from the G-CSF- or the saline-treated mice assessed by flow cytometric analysis. The total cell number of $CD4^+CD25^+$ Tregs was counted in spleen (B) and inguinal lymph nodes (C) after G-CSF treatment. *$P<0.05$. #$P<0.01$. The means ± SEM of 6 animals are shown.

mice compared with the saline-treated mice (G-CSF group: 8.7 ± 4.9 cells/mm^2 vs. saline group: 2.8 ± 3.6 cells/mm^2, $P<0.05$) (Fig. 5B).

3.5. Involvement of Tregs in G-CSF-induced atheroprotective effects

To confirm whether Tregs were involved in mechanisms of the atheroprotective effects of G-CSF, we examined the effects of G-CSF on Tregs-depleted $ApoE^{-/-}$ mice using PC61. More than 90% of $CD4^+CD25^+$ Tregs were decreased in inguinal lymph nodes at 14 days after a single intraperitoneal injection of 100 μg of PC61 (Fig. 6A). Administration of this antibody every two weeks abolished the protective effects of G-CSF on atherosclerosis. G-CSF significantly reduced the area of Oil Red-O-positive atherosclerotic lesion in $ApoE^{-/-}$ mice, but the Oil Red-O-positive atherosclerotic lesion area was not significantly different between the saline-treated Tregs-depleted $ApoE^{-/-}$ mice (PC61-saline group) and the G-CSF-treated Tregs-depleted $ApoE^{-/-}$ mice (PC61-G-CSF group) (PC61-G-CSF group: $18.0 \pm 2.6 \times 10^4$ μm^2 vs. PC61-saline group: $18.8 \pm 2.3 \times 10^4$ μm^2, $P=0.67$) (Fig. 6B, C). G-CSF significantly reduced the level of IFN-γ and increased the level of IL-10 in $ApoE^{-/-}$ mice, but the levels of IFN-γ and IL-10 also were not different between the PC61-saline group and the PC61-G-CSF group (IFN-γ; PC61-G-CSF group: 37.1 ± 8.0% vs. PC61-saline group: 38.2 ± 8.5%, $P=0.82$, IL-10; PC61-G-CSF group: 5.1 ± 2.6% vs. PC61-saline group: 5.8 ± 1.3%, $P=0.62$) (Fig. 6D, E).

Furthermore, we examined the effects of G-CSF on atherosclerosis using $ApoE^{-/-}/CD28^{-/-}$ double knockout (DKO) mice. In the DKO mice, approximately 90% of $CD4^+CD25^+$ Tregs were decreased in inguinal lymph nodes (Fig. 7A). The treatment with G-CSF did not reduce the atherosclerotic lesion area in the DKO mice (G-CSF group: $17.8 \pm 0.9 \times 10^4$ μm^2 vs. saline group: $17.5 \pm 1.8 \times 10^4$ μm^2, $P=0.67$) (Fig. 7B). The levels of IFN-γ and IL-10 were not different between the saline group and the G-CSF group (IFN-γ; G-CSF group: 31.3 ± 3.8% vs. saline group: 31.3 ± 1.5%, $P=0.99$, IL-10; G-CSF group: 6.3 ± 0.5% vs. saline group: 6.2 ± 0.9%, $P=0.86$) (Fig. 7C, D).

4. Discussion

In the present study, we demonstrated that G-CSF prevents the progression of atherosclerosis and that the increased Tregs subset is involved in the atheroprotective mechanism of G-CSF in $ApoE^{-/-}$ mice. Interestingly, the blood lipid concentrations were not significantly different between the G-CSF-treated mice and the saline-treated mice. G-CSF increased the number of Foxp3-positive Tregs in atherosclerotic lesions, along with the decreased level of atherogenic proinflammatory cytokine IFN-γ and the increased level of antiinflammatory cytokine IL-10. Administration of anti-CD25 antibody that depletes Tregs abrogated these atheroprotective effects of G-CSF. The protective effects of G-CSF on atherosclerosis were not recognized in $ApoE^{-/-}/CD28^{-/-}$ double knockout mice. These results suggest that Tregs may play a critical role in the inhibition of atherosclerosis by G-CSF.

The effects of G-CSF on atherosclerosis have been controversial in animal experiments and clinical trials. Previously, we demonstrated that the treatment with G-CSF ameliorates the progression of atherosclerosis using two kinds of rabbit models of atherosclerosis

Please cite this article as: Uchiyama R, et al, Role of regulatory T cells in atheroprotective effects of granulocyte colony-stimulating factor, J Mol Cell Cardiol (2012), doi:10.1016/j.yjmcc.2011.12.016

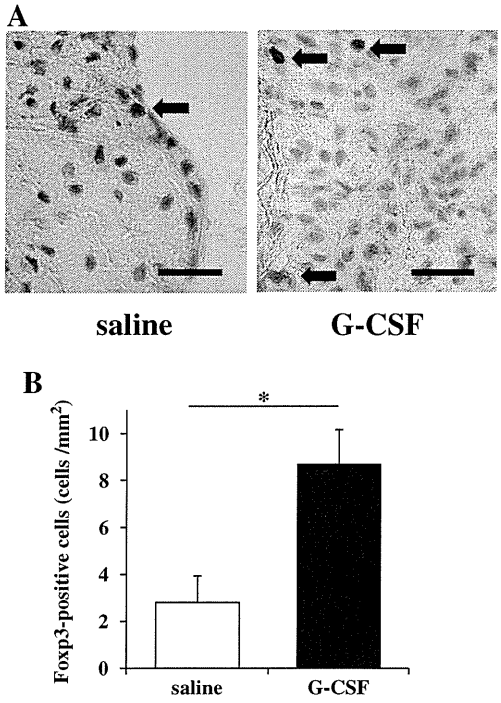

Fig. 5. Effects of G-CSF on Tregs accumulation in atherosclerotic lesion at the aortic sinus. (A) Representative photographs of immunostaining with Foxp3 in the atherosclerotic lesion of the saline-treated mice and the G-CSF-treated mice. Arrows indicate Foxp3-positive cells. (B) The number of Foxp3-positive Tregs in atherosclerosis lesion of the saline-treated and the G-CSF-treated mice. *$P<0.05$. Scale bars indicates 100 μm. The means ± SEM of 10 animals are shown.

[13]. Yoshioka et al. [15] reported that G-CSF treatment accelerated reendothelialization and decreased neointimal formation in mice wire injury model. In contrast, Haghighat et al. [26] showed that G-CSF treatment resulted in the exacerbation of atherosclerosis in ApoE$^{-/-}$ mice. They administered G-CSF subcutaneously to mice at a dose of 10 μg/kg once a day for 5 days per a week on alternating weeks for a total of 20 doses over an 8-week treatment period. The rapid increase and decrease in the number of white blood cell by repeated start and cessation of G-CSF administration may affect the adverse effect on atherosclerosis. Although they showed that G-CSF increases in vessels at adventitia, there is no solid evidence whether the increased vessels at adventitia exacerbate atherosclerosis. Kang et al. [27] reported that G-CSF treatment (10 μg/kg once a day for 4 days before percutaneous coronary intervention (PCI)) increased the risk of in-stent stenosis in patients with acute or old MI. However, number of enrolled patients was small and only a few patients were assessed by coronary angiography at six-month follow-up in the study. Additionally, patients did not receive primary PCI during the golden time of acute MI treatment and PCI was performed under the condition of increasing number of leukocytes by G-CSF. In our clinical trial, G-CSF treatment (2.5 μg/kg once a day for 5 days after PCI) did not affect the restenosis rate in patients with acute MI [12]. Moreover, other randomized clinical trials also reported that G-CSF did not increase the restenosis rate after PCI [28].

The pathogenesis of atherosclerosis is associated with chronic inflammatory mechanisms. The atherosclerotic plaque is characterized by an accumulation of lipids in the artery wall, together with infiltration of immunocytes, such as macrophages, T cells, and mast cells. An increasing body of evidence suggests that the immune system is involved in the process of atherosclerosis [29,30]. T cells are recruited in parallel with macrophages in atherosclerotic lesions and produce proatherogenic mediators. IFN-γ, the signature Th1 cytokine, is present in the human plaque and has pathogenic effects on atherosclerosis [31]. IL-4, the signature Th2 cytokine, is not frequently observed in human plaques, and experimental studies examining the involvement of Th2 cells are contradictory [32]. Several studies have demonstrated a protective effect of Tregs in models of atherosclerosis. CD4$^+$CD25$^+$ Tregs are specialized for the suppression of both Th1 and Th2 pathogenic immune responses against self or foreign antigens and control T cell homeostasis. There has been accumulated evidence indicating that Tregs exert important regulatory functions in various immuno-inflammatory diseases [33]. Tregs play an important role in preventing the spontaneous development of systemic autoimmunity through IL-10 and TGF-β. Zouggari et al. [34] reported that Tregs deletion significantly enhanced postischemic neovascularization by increasing the levels of proinflammatory cytokines. Shi et al. [35] reported that adoptive transfer of Tregs ameliorated coxsackievirus B3-induced myocarditis through suppression of the immune response to heart. TGF-β and phosphorylated Akt levels were upregulated and coxsackie-adenovirus receptor expression was decreased in the heart of the Tregs-transferred mice compared with those in the control mice. Tregs inhibit the functions of activated helper T cells through cell-to-cell contact and soluble inhibitory cytokines such as IL-10 and TGF-β [36]. TGF-β and IL-10 produced by Tregs are reported to have profound atheroprotective effects in mouse models.

G-CSF is a hematopoietic cytokine that stimulates the proliferation and differentiation of normal hematopoietic stem cells. G-CSF mediates immune regulation by inducing apoptosis of T cells and inhibiting proliferation of T cells in response to mitogens [37]. G-CSF stimulation alters the T cell function and modulates the balance between Th1 and Th2 immune responses by affecting cytokine production [17,38]. G-CSF suppresses the productions of proinflammatory cytokines stimulated by lipopolysaccharide in whole blood cells and monocytes [39,40]. In addition to these immune effects, G-CSF mobilizes bone marrow CD4$^+$CD25$^+$ Tregs via reducing the expression of stromal-derived factor in the bone marrow and changing CD4$^+$CD25$^+$ Tregs trafficking [41]. Therefore, we examined whether Tregs are involved in the atheroprotective mechanism of G-CSF. In the present study, G-CSF increased the number of Tregs in spleen and peripheral lymph nodes, and atherosclerotic lesion. Moreover, G-CSF increased the level of IL-10 and decreased the level of IFN-γ in atherosclerotic lesion. IL-10 is reported to inhibit the production of proinflammatory cytokines such as IFN-γ in T cells [36]. These results suggest that G-CSF prevents the progression of atherosclerosis by recruiting Tregs and increasing IL-10 level in plaque. To address the question whether Tregs were implicated in the mechanism of G-CSF-mediated atheroprotective effect, we used two types of Tregs-depleted ApoE$^{-/-}$ mice, which are ApoE$^{-/-}$ mice injected with Treg-depleting antibody (PC61) and ApoE$^{-/-}$/CD28$^{-/-}$ mice. Costimulatory molecule CD28 is required for the generation and homeostasis of Tregs and the number of Tregs is reduced in CD28-deficient mice [22]. Noteworthy, G-CSF treatment exerted no atheroprotective effects in both types of Tregs-depleted ApoE$^{-/-}$ mice. G-CSF-induced decrease in IFN-γ and increase in IL-10 in atherosclerotic plaque were abrogated in Tregs-depleted ApoE$^{-/-}$ mice. These findings suggest that Tregs play an important role in the atheroprotective effects of G-CSF. Some studies reported that TGF-β is a critical mediator of Tregs and others showed that IL-10 is a key molecule of Tregs [3,42,43]. In the present study, TGF-β mRNA in atherosclerotic plaque was not increased by G-CSF, however, we could not exclude the possibility that TGF-β is involved in the G-CSF-induced atheroprotective effect. As some agents including statins and angiotensin-converting enzyme inhibitors are reported to expand Tregs *in vivo* [44,45] modulation of Tregs may become a promising therapeutic target to prevent cardiovascular diseases.

In conclusion, our results demonstrate that G-CSF prevents the progression of atherosclerosis and the increased Tregs are involved in the atheroprotective mechanism of G-CSF in ApoE$^{-/-}$ mice. Further studies including clinical trials are needed to clarify the feasibility and safety of G-CSF-induced atheroprotective effect. In the future, manipulating Tregs by G-CSF or biological agents may provide novel therapeutic strategies for atherosclerosis.

Please cite this article as: Uchiyama R, et al, Role of regulatory T cells in atheroprotective effects of granulocyte colony-stimulating factor, J Mol Cell Cardiol (2012), doi:10.1016/j.yjmcc.2011.12.016

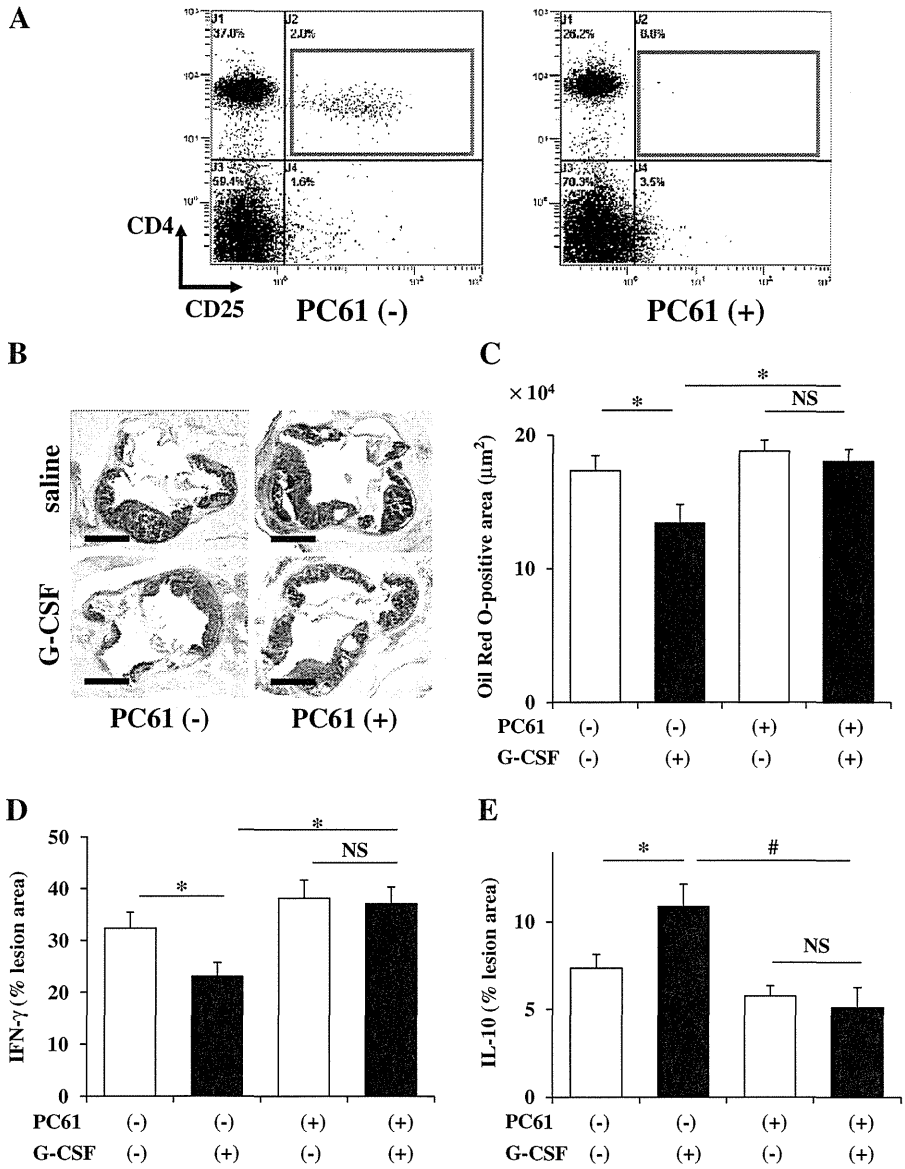

Fig. 6. Atheroprotective effects of G-CSF were abrogated in Tregs-depleted ApoE$^{-/-}$ mice. (A) The proportions of CD4^{+}CD25^{+} Tregs in inguinal lymph nodes from the PC61 or the PBS-treated mice assessed by flow cytometric analysis. (B) Representative photographs of the atherosclerotic lesion formation at the aortic sinus of the saline-treated ApoE$^{-/-}$ mice, the G-CSF-treated ApoE$^{-/-}$ mice, the saline and PC61-treated ApoE$^{-/-}$ mice and the G-CSF and PC61-treated ApoE$^{-/-}$ mice. Sections were taken at the same level of aortic sinus and stained with Oil Red-O as described in Materials and methods. (C) Quantitative analysis of atherosclerotic lesion formation at the aortic sinus in each group. The average lesion area of five sections at the aortic sinus from each mouse was quantified morphometrically after 4 weeks of saline or G-CSF treatment as described in Materials and methods. (D) Quantitative analysis of the level of IFN-γ in atherosclerotic plaque of the Tregs-depleted ApoE$^{-/-}$ mice. (E) Quantitative analysis of the level of IL-10 in atherosclerotic plaque of the Tregs-depleted ApoE$^{-/-}$ mice. $^{*}P<0.05$. $^{\#}P<0.01$. NS indicates that there is no significant difference between the two groups. Scale bars indicates 400 μm. The means ± SEM of 10 animals are shown.

Disclosures

The authors confirm that there are no conflicts of interest.

Acknowledgments

This work was supported by grants from the Ministry of Health Labour and Welfare in Japan and SENSHIN Medical Research Foundation. The authors thank Ryo Abe (Research Institute for Biological Sciences, Science University of Tokyo, Chiba, Japan) for kindly gift of CD28$^{-/-}$ mice. The authors also thank Akane Furuyama, Yuko Ohtsuki, Megumi Ikeda, Ikuko Sakamoto, Megumi Iiyama and Miho Kikuchi for their excellent technical assistance.

References

[1] Galkina E, Ley K. Immune and inflammatory mechanisms of atherosclerosis. Annu Rev Immunol 2009;27:165–97.
[2] Huehn J, Polansky JK, Hamann A. Epigenetic control of FOXP3 expression: the key to a stable regulatory T-cell lineage? Nat Rev Immunol 2009;9:83–9.
[3] Ait-Oufella H, Salomon BL, Potteaux S, Robertson AK, Gourdy P, Zoll J, et al. Natural regulatory T cells control the development of atherosclerosis in mice. Nat Med 2006;12:178–80.
[4] Mallat Z, Gojova A, Brun V, Esposito B, Fournier N, Cottrez F, et al. Induction of a regulatory T cell type 1 response reduces the development of atherosclerosis in apolipoprotein E-knockout mice. Circulation 2003;108:1232–7.
[5] Sakaguchi S. Naturally arising Foxp3-expressing CD25+CD4+ regulatory T cells in immunological tolerance to self and non-self. Nat Immunol 2005;6:345–52.
[6] Takahashi T, Kalka C, Masuda H, Chen D, Silver M, Kearney M, et al. Ischemia- and cytokine-induced mobilization of bone marrow-derived endothelial progenitor cells for neovascularization. Nat Med 1999;5:434–8.

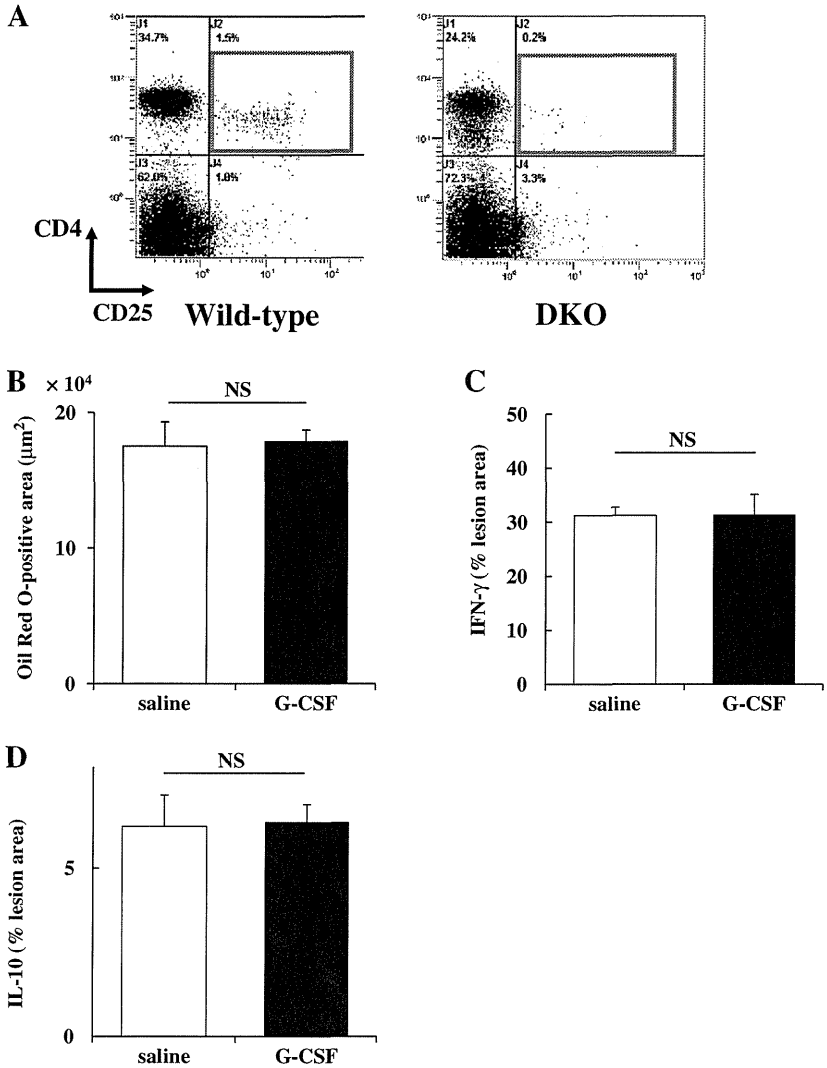

Fig. 7. Atheroprotective effects of G-CSF were abrogated in ApoE$^{-/-}$/CD28$^{-/-}$ mice. (A) The proportions of CD4^{+}CD25^{+} Tregs in inguinal lymph nodes from wild type mice and DKO mice assessed by flow cytometric analysis. (B) Quantitative analysis of atherosclerotic lesion formation at the aortic sinus in ApoE$^{-/-}$/CD28$^{-/-}$ mice. The average lesion area of five sections at the aortic sinus from each mouse was quantified morphometrically after 4 weeks of saline or G-CSF treatment as described in Materials and methods. (C) Quantitative analysis of the level of IFN-γ in atherosclerotic plaque of the DKO mice. (D) Quantitative analysis of the level of IL-10 in atherosclerotic plaque of the DKO mice. NS indicates that there is no significant difference between the two groups. The means ± SEM of 9 animals are shown.

[7] Rutella S, Zavala F, Danese S, Kared H, Leone G. Granulocyte colony-stimulating factor: a novel mediator of T cell tolerance. J Immunol 2005;175:7085–91.
[8] Harada M, Qin Y, Takano H, Minamino T, Zou Y, Toko H, et al. G-CSF prevents cardiac remodeling after myocardial infarction by activating the Jak-Stat pathway in cardiomyocytes. Nat Med 2005;11:305–11.
[9] Ince H, Petzsch M, Kleine HD, Schmidt H, Rehders T, Korber T, et al. Preservation from left ventricular remodeling by front-integrated revascularization and stem cell liberation in evolving acute myocardial infarction by use of granulocyte-colony-stimulating factor (FIRSTLINE-AMI). Circulation 2005;112:3097–106.
[10] Minatoguchi S, Takemura G, Chen XH, Wang N, Uno Y, Koda M, et al. Acceleration of the healing process and myocardial regeneration may be important as a mechanism of improvement of cardiac function and remodeling by postinfarction granulocyte colony-stimulating factor treatment. Circulation 2004;109:2572–80.
[11] Ohtsuka M, Takano H, Zou Y, Toko H, Akazawa H, Qin Y, et al. Cytokine therapy prevents left ventricular remodeling and dysfunction after myocardial infarction through neovascularization. FASEB J 2004;18:851–3.
[12] Takano H, Hasegawa H, Kuwabara Y, Nakayama T, Matsuno K, Miyazaki Y, et al. Feasibility and safety of granulocyte colony-stimulating factor treatment in patients with acute myocardial infarction. Int J Cardiol 2007;122:41–7.
[13] Hasegawa H, Takano H, Ohtsuka M, Ueda K, Niitsuma Y, Qin Y, et al. G-CSF prevents the progression of atherosclerosis and neointimal formation in rabbits. Biochem Biophys Res Commun 2006;344:370–6.
[14] Kong D, Melo LG, Gnecchi M, Zhang L, Mostoslavsky G, Liew CC, et al. Cytokine-induced mobilization of circulating endothelial progenitor cells enhances repair of injured arteries. Circulation 2004;110:2039–46.
[15] Yoshioka T, Takahashi M, Shiba Y, Suzuki C, Morimoto H, Izawa A, et al. Granulocyte colony-stimulating factor (G-CSF) accelerates reendothelialization and reduces neointimal formation after vascular injury in mice. Cardiovasc Res 2006;70:61–9.
[16] Matsumoto T, Watanabe H, Ueno T, Tsunemi A, Hatano B, Kusumi Y, et al. Appropriate doses of granulocyte-colony stimulating factor reduced atherosclerotic plaque formation and increased plaque stability in cholesterol-fed rabbits. J Atheroscler Thromb 2010;17:84–96.
[17] Sloand EM, Kim S, Maciejewski JP, Van Rhee F, Chaudhuri A, Barrett J, et al. Pharmacologic doses of granulocyte colony-stimulating factor affect cytokine production by lymphocytes in vitro and in vivo. Blood 2000;95:2269–74.
[18] Reyes E, Garcia-Castro I, Esquivel F, Hornedo J, Cortes-Funes H, Solovera J, et al. Granulocyte colony-stimulating factor (G-CSF) transiently suppresses mitogen-stimulated T-cell proliferative response. Br J Cancer 1999;80:229–35.
[19] Kared H, Masson A, Adle-Biassette H, Bach JF, Chatenoud L, Zavala F. Treatment with granulocyte colony-stimulating factor prevents diabetes in NOD mice by recruiting plasmacytoid dendritic cells and functional CD4(+)CD25(+) regulatory T-cells. Diabetes 2005;54:78–84.
[20] Liang HL, Yi DH, Zheng QJ, Du JF, Cao YX, Yu SQ, et al. Improvement of heart allograft acceptability associated with recruitment of CD4+CD25+ T cells in peripheral blood by recipient treatment with granulocyte colony-stimulating factor. Transplant Proc 2008;40:1604–11.
[21] Paigen B, Morrow A, Holmes PA, Mitchell D, Williams RA. Quantitative assessment of atherosclerotic lesions in mice. Atherosclerosis 1987;68:231–40.
[22] Shahinian A, Pfeffer K, Lee KP, Kundig TM, Kishihara K, Wakeham A, et al. Differential T cell costimulatory requirements in CD28-deficient mice. Science 1993;261:609–12.

Please cite this article as: Uchiyama R, et al, Role of regulatory T cells in atheroprotective effects of granulocyte colony-stimulating factor, J Mol Cell Cardiol (2012), doi:10.1016/j.yjmcc.2011.12.016

[23] Hu Y, Zhang H, Lu Y, Bai H, Xu Y, Zhu X, et al. Class A scavenger receptor attenuates myocardial infarction-induced cardiomyocyte necrosis through suppressing M1 macrophage subset polarization. Basic Res Cardiol 2011;106:1311–28.
[24] Leucht C, Stigloher C, Wizenmann A, Klafke R, Folchert A, Bally-Cuif L. MicroRNA-9 directs late organizer activity of the midbrain-hindbrain boundary. Nat Neurosci 2008;11:641–8.
[25] Gotsman I, Grabie N, Gupta R, Dacosta R, MacConmara M, Lederer J, et al. Impaired regulatory T-cell response and enhanced atherosclerosis in the absence of inducible costimulatory molecule. Circulation 2006;114:2047–55.
[26] Haghighat A, Weiss D, Whalin MK, Cowan DP, Taylor WR. Granulocyte colony-stimulating factor and granulocyte macrophage colony-stimulating factor exacerbate atherosclerosis in apolipoprotein E-deficient mice. Circulation 2007;115: 2049–54.
[27] Kang HJ, Kim HS, Zhang SY, Park KW, Cho HJ, Koo BK, et al. Effects of intracoronary infusion of peripheral blood stem-cells mobilised with granulocyte-colony stimulating factor on left ventricular systolic function and restenosis after coronary stenting in myocardial infarction: the MAGIC cell randomised clinical trial. Lancet 2004;363:751–6.
[28] Takano H, Ueda K, Hasegawa H, Komuro I. G-CSF therapy for acute myocardial infarction. Trends Pharmacol Sci 2007;28:512–7.
[29] Binder CJ, Chang MK, Shaw PX, Miller YI, Hartvigsen K, Dewan A, et al. Innate and acquired immunity in atherogenesis. Nat Med 2002;8:1218–26.
[30] Hansson GK. Inflammation, atherosclerosis, and coronary artery disease. N Engl J Med 2005;352:1685–95.
[31] Hansson GK, Hermansson A. The immune system in atherosclerosis. Nat Immunol 2011;12:204–12.
[32] Davenport P, Tipping PG. The role of interleukin-4 and interleukin-12 in the progression of atherosclerosis in apolipoprotein E-deficient mice. Am J Pathol 2003;163: 1117–25.
[33] Sakaguchi S, Fukuma K, Kuribayashi K, Masuda T. Organ-specific autoimmune diseases induced in mice by elimination of T cell subset. I. Evidence for the active participation of T cells in natural self-tolerance; deficit of a T cell subset as a possible cause of autoimmune disease. J Exp Med 1985;161:72–87.
[34] Zouggari Y, Ait-Oufella H, Waeckel L, Vilar J, Loinard C, Cochain C, et al. Regulatory T cells modulate postischemic neovascularization. Circulation 2009;120: 1415–25.
[35] Shi Y, Fukuoka M, Li G, Liu Y, Chen M, Konviser M, et al. Regulatory T cells protect mice against coxsackievirus-induced myocarditis through the transforming growth factor beta-coxsackie-adenovirus receptor pathway. Circulation 2010;121:2624–34.
[36] Taleb S, Tedgui A, Mallat Z. Regulatory T-cell immunity and its relevance to atherosclerosis. J Intern Med 2008;263:489–99.
[37] Rutella S, Rumi C, Testa U, Sica S, Teofili L, Martucci R, et al. Inhibition of lymphocyte blastogenic response in healthy donors treated with recombinant human granulocyte colony-stimulating factor (rhG-CSF): possible role of lactoferrin and interleukin-1 receptor antagonist. Bone Marrow Transplant 1997;20:355–64.
[38] Pan L, Delmonte Jr J, Jalonen CK, Ferrara JL. Pretreatment of donor mice with granulocyte colony-stimulating factor polarizes donor T lymphocytes toward type-2 cytokine production and reduces severity of experimental graft-versus-host disease. Blood 1995;86:4422–9.
[39] Boneberg EM, Hareng L, Gantner F, Wendel A, Hartung T. Human monocytes express functional receptors for granulocyte colony-stimulating factor that mediate suppression of monokines and interferon-gamma. Blood 2000;95:270–6.
[40] Boneberg EM, Hartung T. Granulocyte colony-stimulating factor attenuates LPS-stimulated IL-1beta release via suppressed processing of proIL-1beta, whereas TNF-alpha release is inhibited on the level of proTNF-alpha formation. Eur J Immunol 2002;32:1717–25.
[41] Zou L, Barnett B, Safah H, Larussa VF, Evdemon-Hogan M, Mottram P, et al. Bone marrow is a reservoir for CD4+CD25+ regulatory T cells that traffic through CXCL12/CXCR4 signals. Cancer Res 2004;64:8451–5.
[42] Kinsey GR, Sharma R, Huang L, Li L, Vergis AL, Ye H, et al. Regulatory T cells suppress innate immunity in kidney ischemia-reperfusion injury. J Am Soc Nephrol 2009;20: 1744–53.
[43] Liesz A, Suri-Payer E, Veltkamp C, Doerr H, Sommer C, Rivest S, et al. Regulatory T cells are key cerebroprotective immunomodulators in acute experimental stroke. Nat Med 2009;15:192–9.
[44] Mira E, Leon B, Barber DF, Jimenez-Baranda S, Goya I, Almonacid L, et al. Statins induce regulatory T cell recruitment via a CCL1 dependent pathway. J Immunol 2008;181: 3524–34.
[45] Platten M, Youssef S, Hur EM, Ho PP, Han MH, Lanz TV, et al. Blocking angiotensin-converting enzyme induces potent regulatory T cells and modulates TH1- and TH17-mediated autoimmunity. Proc Natl Acad Sci U S A 2009;106:14948–53.

Please cite this article as: Uchiyama R, et al, Role of regulatory T cells in atheroprotective effects of granulocyte colony-stimulating factor, J Mol Cell Cardiol (2012), doi:10.1016/j.yjmcc.2011.12.016

Cell Metabolism
Article

p53-Induced Adipose Tissue Inflammation Is Critically Involved in the Development of Insulin Resistance in Heart Failure

Ippei Shimizu,[1,5] Yohko Yoshida,[1,5] Taro Katsuno,[1] Kaoru Tateno,[1] Sho Okada,[1] Junji Moriya,[1] Masataka Yokoyama,[1] Aika Nojima,[1] Takashi Ito,[1] Rudolf Zechner,[2] Issei Komuro,[3] Yoshio Kobayashi,[1] and Tohru Minamino[1,4,*]
[1]Department of Cardiovascular Science and Medicine, Chiba University Graduate School of Medicine, Chiba 260-8670, Japan
[2]Institute of Molecular Biosciences, University of Graz, A-8010 Graz, Austria
[3]Department of Cardiovascular Medicine, Osaka University School of Medicine, Osaka 565-0871, Japan
[4]PRESTO, Japan Science and Technology Agency, Saitama 332-0012, Japan
[5]These authors contributed equally to this work
*Correspondence: t_minamino@yahoo.co.jp
DOI 10.1016/j.cmet.2011.12.006

SUMMARY

Several clinical studies have shown that insulin resistance is prevalent among patients with heart failure, but the underlying mechanisms have not been fully elucidated. Here, we report a mechanism of insulin resistance associated with heart failure that involves upregulation of p53 in adipose tissue. We found that pressure overload markedly upregulated p53 expression in adipose tissue along with an increase of adipose tissue inflammation. Chronic pressure overload accelerated lipolysis in adipose tissue. In the presence of pressure overload, inhibition of lipolysis by sympathetic denervation significantly downregulated adipose p53 expression and inflammation, thereby improving insulin resistance. Likewise, disruption of p53 activation in adipose tissue attenuated inflammation and improved insulin resistance but also ameliorated cardiac dysfunction induced by chronic pressure overload. These results indicate that chronic pressure overload upregulates adipose tissue p53 by promoting lipolysis via the sympathetic nervous system, leading to an inflammatory response of adipose tissue and insulin resistance.

INTRODUCTION

The p53 tumor suppressor pathway coordinates DNA repair, cell-cycle arrest, apoptosis, and senescence to preserve genomic stability and prevent oncogenesis. Activation of p53 is driven by a wide variety of stress signals that have the potential to promote tumor formation, such as DNA damage, telomere shortening, oxidative stress, and oncogene activation (Harris and Levine, 2005; Meek, 2009; Vousden and Prives, 2009). Recently, the contribution of p53 to many undesirable aspects of aging and age-associated diseases, such as cardiovascular and metabolic disorders, has been recognized (Royds and Iacopetta, 2006; Vousden and Lane, 2007). It has been reported that aging is associated with an increase of the p53-mediated transcriptional activity (Edwards et al., 2007) and that slight constitutive overactivation of p53 is associated with premature aging in mice (Maier et al., 2004; Tyner et al., 2002). Activation of p53 has also been observed in aged vessels and failing hearts and has been implicated in atherosclerosis and heart failure (Minamino and Komuro, 2007, 2008; Sano et al., 2007). Recent findings have indicated a role of p53 in determining the response of cells to nutrient stress and in regulating metabolism (Vousden and Ryan, 2009). It has also been demonstrated that excessive calorie intake induces p53-induced inflammation in adipose tissue, leading to insulin resistance and diabetes in mice (Minamino et al., 2009).

A close link between heart failure and diabetes has long been recognized in the clinical setting (Ashrafian et al., 2007; Lopaschuk et al., 2007; Witteles and Fowler, 2008). Many mechanisms have been suggested to explain the increased incidence of heart failure in diabetic patients, including the hypertrophic influence of insulin, the adverse effects of hyperglycemia, increased oxidative stress, and hyperactivity of neurohumoral systems, such as the renin-angiotensin-aldosterone system and the adrenergic system. Recently, increasing attention has been paid to insulin resistance as a distinct cause of cardiac dysfunction and heart failure in diabetic patients. A study of Swedish patients without prior cardiac dysfunction found that insulin resistance predicted the subsequent onset of heart failure independently of established risk factors (Ingelsson et al., 2005). In another clinical study, the plasma level of proinsulin (a marker of insulin resistance) was found to be higher in patients who subsequently developed heart failure than in control patients 20 years before the actual diagnosis of heart failure (Arnlöv et al., 2001). These findings indicate that insulin resistance precedes heart failure rather than being a consequence of it. Evidence has emerged that myocardial insulin resistance is central to altered metabolism in the failing heart and may play a crucial role in the development of heart failure (Ashrafian et al., 2007; Lopaschuk et al., 2007; Witteles and Fowler, 2008). The adaptive response of the failing heart involves a complex series of enzymatic shifts and changes in the regulation of transcriptional factors, which result in an increase of glucose metabolism and a decrease of fatty acid metabolism

to maximize the efficacy of energy production (Neubauer, 2007). Insulin resistance of the myocardium inhibits these adaptive responses, leading to increased reliance on fatty acid metabolism. This increases oxygen consumption and decreases cardiac function, raising the potential for lipotoxicity in the heart (Sharma et al., 2007; Young et al., 2002). Another line of evidence indicates that insulin signaling is upregulated in the failing heart and that excessive cardiac insulin signaling exacerbates systolic dysfunction (Shimizu et al., 2010).

Moreover, there is increasing evidence that heart failure reciprocally augments the risk of insulin resistance and clinical diabetes (Ashrafian et al., 2007). Insulin resistance and abnormal glucose metabolism are very common in heart failure patients, being identified in 43% of these patients, and such abnormalities are associated with decreased cardiac function (Suskin et al., 2000). Surprisingly, the link between heart failure and insulin resistance grows stronger when patients with ischemic heart disease are excluded (Witteles and Fowler, 2008). Heart failure also predicts the development of type 2 diabetes in a graded way (Tenenbaum et al., 2003). Although the above mentioned clinical evidence supports a role of insulin resistance in the occurrence of heart failure, evidence for the reciprocal statement that heart failure promotes insulin resistance is largely associative. Moreover, the role of heart failure in the promotion of insulin resistance has been demonstrated by only a few animal studies (Nikolaidis et al., 2004; Shimizu et al., 2010) and the underlying mechanisms are largely speculative.

Here, we studied the role of heart failure in the development of insulin resistance and sought to elucidate the molecular mechanisms involved. We found that insulin resistance developed in two murine models of heart failure, a chronic pressure overload model and a myocardial infarction model. Heart failure markedly upregulated p53 expression in adipose tissue in association with increased inflammation of adipose tissue. Heart failure accelerated lipolysis in adipose tissue, whereas inhibition of lipolysis by sympathetic denervation or treatment with a lipase inhibitor significantly downregulated adipose tissue p53 expression and inflammation, thereby improving insulin resistance. Likewise, disruption of p53 activation in adipose tissue not only ameliorated inflammation in this tissue and improved insulin resistance but also improved cardiac dysfunction associated with heart failure. We conclude that heart failure upregulates p53 in adipose tissue by promoting lipolysis via activation of the sympathetic nervous system, leading to an inflammatory response of adipose tissue and insulin resistance. Our results indicate that inhibition of p53-induced adipose inflammation is a potential target for treating metabolic abnormalities and systolic dysfunction in patients with heart failure.

RESULTS

Pressure Overload Induces Adipose Tissue Inflammation and Insulin Resistance

To examine the effect of cardiac pressure overload on glucose homeostasis, we produced transverse aortic constriction (TAC) in 11-week-old mice. In this mouse model, systolic cardiac function deteriorated significantly along with left ventricular (LV) dilatation 2–6 weeks after surgery (Figure S1A available online). The insulin tolerance test (ITT) and the glucose tolerance test (GTT) showed that insulin sensitivity and glucose tolerance were impaired at 4–6 weeks after TAC (Figure 1A) without any change of food intake (Figure S1B). In patients with metabolic disorders, the recruitment of inflammatory macrophages to adipose tissue has been shown to increase the production of proinflammatory cytokines, such as tumor necrosis factor (TNF)-α and chemokine (C–C motif) ligand 2 (CCL2), also known as monocyte chemoattractant protein-1 (MCP-1), leading to the development of systemic insulin resistance (Hotamisligil et al., 1993; Kamei et al., 2006; Weisberg et al., 2003). Therefore, we investigated whether pressure overload provokes adipose tissue inflammation. Examination of hematoxylin- and eosin-stained sections demonstrated the infiltration of mononuclear cells into visceral fat, with most of these cells being identified as macrophages by immunofluorescent staining for Mac3 (Figure 1B). Consistent with these results, expression of a marker for macrophages (Egf-like module containing, mucin-like, hormone receptor-like 1; EMR1) and production of proinflammatory cytokines were significantly upregulated in the adipose tissue of TAC mice along with a decrease of adiponectin (Figure 1C) compared with sham-operated mice. Treatment of TAC mice with a neutralizing antibody for Tnf-α significantly improved insulin resistance and glucose intolerance, suggesting a crucial role in the upregulation of proinflammatory cytokines in the development of metabolic abnormalities during heart failure (Figure S1C).

Pressure Overload Increases Lipolysis and Induces p53-Dependent Inflammation in Adipose Tissue during Heart Failure

Computed tomography (CT) showed a significant decrease of visceral fat after the creation of pressure overload (Figure 1D). It is well accepted that sympathetic activity increases with heart failure (Floras, 2009), and norepinephrine regulates lipolysis in adipose tissue. We found that the norepinephrine levels of plasma and adipose tissue increased significantly and plasma fatty acid levels were markedly elevated in TAC mice compared with sham-operated mice, suggesting acceleration of lipolysis via the sympathetic nervous system in response to pressure overload (Figure 1E). It has been reported that exposure to an excess of fatty acids leads to p53 activation in various cells (Zeng et al., 2008) and that p53 is crucially involved in the regulation of adipose tissue inflammation in obese animals (Minamino et al., 2009). Therefore, we hypothesized that chronic pressure overload promotes lipolysis and the resultant increase of fatty acids leads to p53-induced inflammation in adipose tissue.

Consistent with this concept, we found that p53 expression was upregulated in the adipose tissue of TAC mice at 2–4 weeks after surgery and the change was sustained until 6 weeks (Figures 2A and S2A). To further investigate the role of adipose tissue p53 in the response to pressure overload, we performed TAC in adipocyte-specific p53 knockout (adipo-p53 KO) mice. The pressure overload-induced increase of p53 expression was attenuated in adipo-p53 KO mice compared with littermate controls (Figure S2B). Production of proinflammatory cytokines as well as cyclin-dependent kinase inhibitor 1A (*Cdkn1a*) expression was also decreased in adipo-p53 KO mice, along with a decline in the infiltration of macrophages into visceral fat

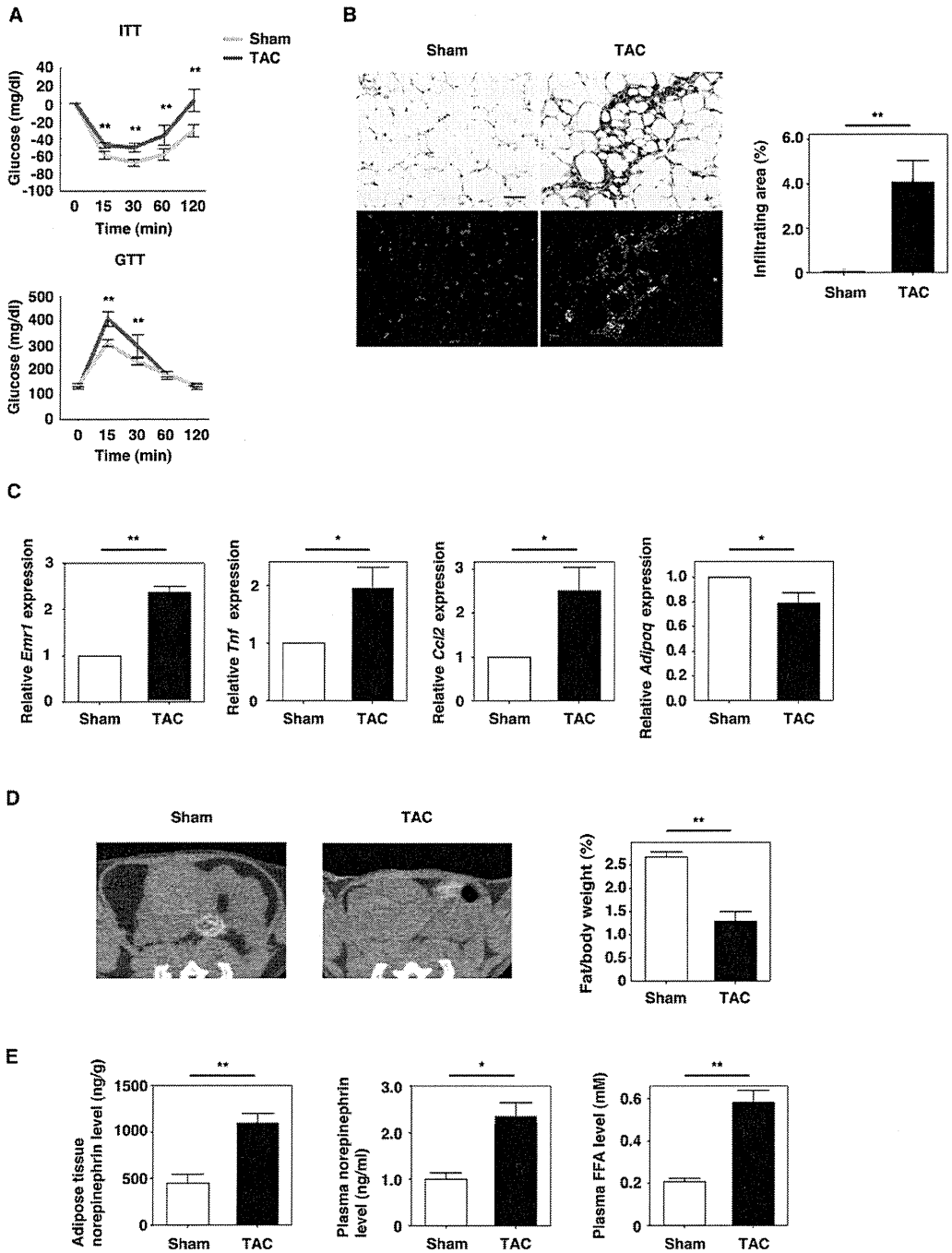

Figure 1. Pressure Overload Induces Systemic Insulin Resistance and Adipose Tissue Lipolysis and Inflammation

(A) Insulin tolerance test (ITT) and glucose tolerance test (GTT) in mice at 6 weeks after sham operation (Sham) or TAC (n = 30).

(B) Hematoxylin and eosin staining of adipose tissues of mice at 6 weeks after sham operation (Sham) or TAC (upper panel). In the lower panel, the infiltration of macrophages was evaluated by immunofluorescent staining for Mac3 (green). Nuclei were stained with Hoechst dye (blue). Scale bar, 50 μm. The right graph indicates the quantitative data on the infiltration of macrophages (n = 5).

(C) Real-time PCR assessing the expression of *Emr1*, *Tnf* (Tnfα), *Ccl2* (MCP1), and *Adipoq* (Adiponectin) levels in adipose tissues of mice at 6 weeks after sham operation (Sham) or TAC (n = 10).

(D) CT analysis of mice at 6 weeks after sham operation (Sham) or TAC. The graph shows the ratio of visceral fat tissue weight estimated by CT to whole body weight (n = 7).

(E) Norepinephrine level in adipose tissue (left) and plasma (middle), and plasma free fatty acid (FFA) level (right) of mice at 6 weeks after sham operation (Sham) or TAC (n = 10). Data are shown as the means ± S.E.M. *p < 0.05, **p < 0.01.